Journal of Computer-Aided Molecular Design, **15:** 935–960, 2001.
KLUWER/ESCOM

Functional group placement in protein binding sites: a comparison of GRID and MCSS

Ryan Bitetti-Putzer[a,b,c], Diane Joseph-McCarthy[b,d,*], James M. Hogle[a,c] & Martin Karplus[a,b,e,*]

[a]*Committee on Higher Degrees in Biophysics, Harvard University, Cambridge, MA 02138, USA;* [b]*Department of Chemistry and Chemical Biology, Harvard University, Cambridge, MA 02138, USA;* [c]*Department of Biological Chemistry and Molecular Pharmacology, Harvard Medical School, Boston, MA 02115, USA;* [d]*Wyeth Research, Biological Chemistry Department, 87 CambridgePark Drive, Cambridge, MA 02140, USA;* [e]*Laboratoire de Chimie Biophysique, ISIS, Université Louis Pasteur, 67000 Strasbourg, France*

Received 24 January 2001; accepted 2 August 2001

Summary

One approach to combinatorial ligand design begins by determining optimal locations (i.e., local potential energy minima) for functional groups in the binding site of a target macromolecule. MCSS and GRID are two methods, based on significantly different algorithms, which are used for this purpose. A comparison of the two methods for the same functional groups is reported. Calculations were performed for nonpolar and polar functional groups in the internal hydrophobic pocket of the poliovirus capsid protein, and on the binding surface of the src SH3 domain. The two approaches are shown to agree qualitatively; i.e., the global characteristics of the functional group maps generated by MCSS and GRID are similar. However, there are significant differences in the relative interaction energies of the two sets of minima, a consequence of the different functional form used to evaluate polar interactions (electrostatics and hydrogen bonding) in the two methods. The single sphere representation used by GRID affords only positional information, supplemented by the identification of hydrogen bonding interactions. By contrast, the multi-atom representation of most MCSS groups yields in both positional and orientational information. The two methods are most similar for small functional groups, while for larger functional groups MCSS yields results consistent with GRID but superior in detail. These results are in accord with the somewhat different purposes for which the two methods were developed. GRID has been used mainly to introduce functionalities at specific positions in lead compounds, in which case the orientation is predetermined by the structure of the latter. The orientational information provided by MCSS is important for its use in the *de novo* design of large, multi-functional ligands, as well as for improving lead compounds.

Introduction

One combinatorial approach to computational ligand design involves the following three steps: (i) determination of the optimal binding sites for various chemical fragments or functional groups; (ii) connection of these functional group sites to form candidate ligands or to modify existing ligands; (iii) estimation of the binding affinities of the proposed ligands. GRID [1–4] and MCSS [5–8] are two methods for finding functional group binding sites, the first step in this process. GRID determines the interaction energy of a chemical fragment or 'probe' at points on an orthogonal grid which encloses the structure of a target macromolecule; it thereby can be used to generate a contour map, similar in spirit to an electron density map, which indicates favorable locations for the probe. This method has been used to find crystallographic positions of some ligands and of bound water molecules, to improve lead compounds such as neuraminidase inhibitors [9, 10] and in the *de novo* design of a thymidylate synthase inhibitor [11]. The GRID

*To whom correspondence should be addressed. E-mail: djoseph@genetics.com; marci@tammy.harvard.edu

library of fragments is based upon probes that can be represented as single spheres and which therefore provide only positional information. A few 'multi-atom' probes have been added to the library, and these are studied by combining the results for the constituent single sphere probes (e.g., carboxylate, for which a single oxygen is anchored at each grid point, and another oxygen is rotated to obtain a best fit). Similarly, the newly added GROUP module [12], designed to deal with molecular probes, works by fitting the results for several single sphere maps; e.g., glucose can be modelled by using the maps for the aliphatic hydroxyl and ether oxygen probes. The MCSS method energy minimizes functional groups, described by an atomic model (rather than a spherical probe model), in Cartesian space and calculates the interaction energy of the group at each local minimum in the target structure. No grid is used in MCSS to speed up the calculation, though it could be, particularly with a Monte Carlo procedure for the minimization (Bitetti-Putzer, et al., work in progress). The present version of MCSS randomly distributes multiple copies (1000 or so) of a given functional group over a specified binding region of a macromolecular target; these copies then are simultaneously and independently energy minimized, resulting in a map of preferred functional group sites. MCSS allows the fully flexible group copies to move in response to the force field of the protein and hence complex functional groups can be studied in the binding site. Thus, detailed orientational, as well as positional, information is obtained. MCSS groups typically are multi-atom structures, in which individual atoms are represented explicitly. These features of the MCSS method are important for the second step in the design process, namely, for joining together the functional groups in the *de novo* computational design of ligands. Ligand design studies have demonstrated the value of both methods [10, 13]. A direct comparison of the MCSS and GRID methods is thus of considerable interest as a means of determining the utility of the two approaches.

The poliovirus capsid was chosen as the primary system for this comparative study, in part because the MCSS method already had been applied to it [13]. Crystal structures of poliovirus and other picornaviruses show that they contain a deep hydrophobic pocket, which binds a number of antiviral drugs known to inhibit infectivity in cell culture-based assays [14–22]. For several of these drugs, crystal structures of the drug complexed with various strains of poliovirus are available [16]. Prior MCSS-based design studies [13] generated a series of candidate ligands that are structurally unrelated to previously existing drugs. Combinatorial libraries of these ligands have been synthesized and several ligands have been shown to bind in biological assays [32] as well crystallographically (Joseph-McCarthy et al., in press). The src SH3 domain [23] was selected as a second model system because this structure has a shallow, exposed binding site, very different from that of the poliovirus capsid protein. SH3 domains normally bind proline-rich sequences in peptides and proteins.

In this report we present the first detailed comparison of GRID and MCSS, and provide information on the advantages and limitations of each method.

Materials and methods

Preparation of protein coordinate files

The native P3/Sabin poliovirus structure (pdb code 1PVC) [14] is refined to a resolution of 2.4 Å with fifteen-fold non-crystallographic redundancy. The R-factor for all data is 0.205. The structure of P3/Sabin complexed with the Janssen compound R78206 (pdb code 1VBA) [16] is refined to 2.9 Å with fifteen-fold non-crystallographic redundancy, and has an R-factor of 0.297 for all data. Comparison of structures refined at this level shows that atoms in identical positions are on the order of 0.2–0.3 Å apart using independently refined structures [15]. The src SH3 domain structure (pdb code 1NLO) [23] is a minimized average structure determined by NMR. The CHARMM potential [26] was used to refine all of these structures, and also is the potential used in MCSS calculations.

A binding region (Figure 1) in the poliovirus capsid protein was determined as described elsewhere [13]. This region encompasses the previously characterized drug binding site (which normally binds a natural ligand, modelled as sphingosine) and extends approximately 12.5 Å beyond any atom of sphingosine. It thus consists of most of the four viral proteins (VP1 to VP4) of one protomer, as well as parts of VP1, VP3, and VP4 of an adjacent protomer; the ligand and the crystal waters are not included. Coordinate files were prepared for the native P3/Sabin structure and for the structure of P3/Sabin complexed with the Janssen compound R78206. The viral protein termini were patched consistent with the crystal structure and the N-terminus of VP4 was myristoylated. Hydrogens were added using the PARAM22 parameter set [24]

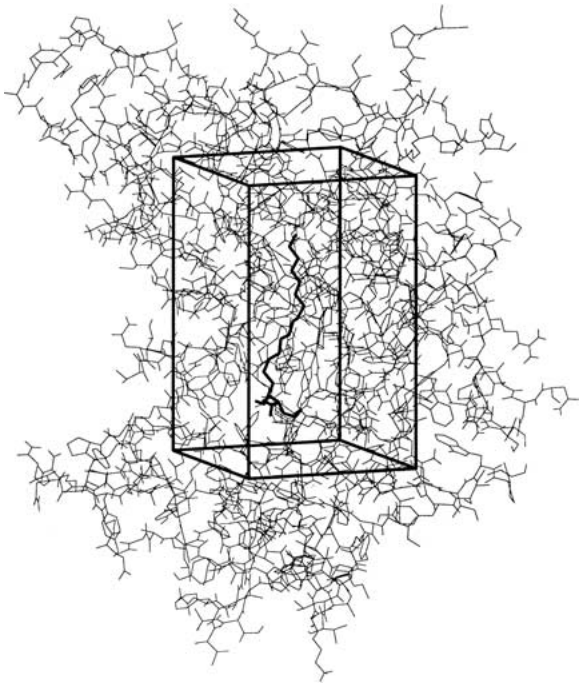

Figure 1. The region of the P3/Sabin poliovirus structure included in the cutout, showing the location of the binding site box used in the initial placement of MCSS group copies; the position of the sphingosine in the native structure also is shown (cf. Joseph-McCarthy et al., 1997).

with the HBUILD command [25] in CHARMM [26]. The region consists of 412 residues and 6452 atoms, including hydrogens. For the src SH3 domain [23], residues 9 through 64 of the NMR structure (including experimental hydrogen positions) were used; it consists of 876 atoms, including hydrogens. The coordinate files prepared for the calculations then were used as the input for program GRIN [1], which is a part of the GRID program suite. GRIN examines all possible hydrogen bonding hydrogens and, if necessary, modifies their positions according to its standard geometry algorithm; no modifications were required for these coordinate files.

GRID calculations

The GRID method [1] was used to determine the interaction energies of various probes at points on an orthogonal grid extending throughout the target protein, or a part of it. The grid spacing was set at 0.5 Å. For poliovirus, GRID map calculations were performed using a 'binding site' box centered on the MCSS placement box (Figure 1) and exceeding it by 2 Å in each dimension (thus $23 \times 21 \times 33$ Å^3). This box encompasses the final energy-minimized positions of most MCSS minima. The entire structure shown in Figure 1, however, is used to determine the interaction energies at each point on this smaller grid. For the src SH3 calculations, the default box determined by GRID surrounds the entire protein structure with a distance of at least 5 Å beyond any protein atom ($40 \times 37 \times 38$ Å^3), and is somewhat larger than the MCSS placement box.

The standard GRID energy function (Figure 2) and parameters [1] were used to calculate the interaction energies. The GRID energy function includes three terms that describe the nonbonded interactions between the probe and the protein: an electrostatic term with a distance-dependent dielectric constant which increases as the probe moves away from the interior; a van der Waals term; and an explicit hydrogen bonding term which, when applied, causes the associated positive van der Waals energy to be neglected. These three terms in GRID parallel those found in the original CHARMM energy function [26] and indeed the parameterization of GRID was based upon the extended atom force field used in that version [1]. The standard GRID parameter values were used to characterize protein hydrogens. GRIN divides hydrogens into two groups based on their ability to participate in hydrogen bonds. The polar hydrogens receive a smaller van der Waals radius and a larger polarizability than the nonpolar hydrogens. All GRID probes examined in this paper are modelled as single spheres and thus only external nonbonded interactions are possible; most probes consist of a single heavy atom with one or more implicit hydrogens. Consequently, GRID calculations using an all-hydrogen protein coordinate file are most analogous to MCSS calculations using the hybrid scheme (see below) and, more particularly, to MCSS calculations in which only the external nonbonded terms are considered. Unless otherwise indicated, the standard GRID truncation scheme was applied, which neglects van der Waals interactions beyond 8 Å and hydrogen bonding interactions beyond 5 Å (i.e., no smoothing function is involved) and which includes all electrostatic interactions regardless of distance.

The GRID probes are represented as single spheres. Thus, a methane probe is modelled as a carbon center, the electronic and spatial properties of which reflect the implicit presence of four associated hydrogens. It is characterized by a partial atomic charge, and by three parameters (the effective number of electrons, polarizability, and van der Waals radius)

CHARMM Energy Function

$$U = U_b + U_\theta + U_\phi + U_w + U_{vdw} + U_{elec}$$

Internal Energy Terms

Bond Potential

$$U_b = \sum k_b (r - r_0)^2$$

Bond Angle Potential

$$U_\theta = \sum k_\theta (\theta - \theta_0)^2$$

Torsion Potential

$$U_\phi = \sum \left| k_\phi \right| - k_\phi \cos(n\phi), \quad \text{n} = 1,2,3,4,6$$

Improper Torsion Potential

$$U_\omega = \sum k_\omega (\omega - \omega_0)^2$$

Nonbonded Energy Terms

Van der Waals Potential

$$U_{vdw} = \sum_{i>j=1} \left(\frac{A_{ij}}{r_{ij}^{12}} - \frac{B_{ij}}{r_{ij}^{6}} \right) sw\left(r_{ij}^2, r_{on}^2, r_{off}^2 \right)$$

Electrostatic Potential

$$U_{elec} = \sum_{i>j=1} \frac{q_i q_j}{\varepsilon r_{ij}}$$

GRID Energy Function

$$E_{xyz} = \sum E_{LJ} + E_{elec} + E_{hb}$$

$$E_{LJ} = \frac{A}{d^{12}} - \frac{B}{d^6}$$

$$E_{elec} = \frac{q_1 q_2}{K\zeta} \left[\frac{1}{d} - \frac{(\zeta - \varepsilon)/(\zeta + \varepsilon)}{\sqrt{d^2 + 4 s_p s_q}} \right]$$

ζ is the dielectric of the protein interior and ε of the water; s_p and s_q are measures of the nominal depths (ref. 1)

$$E_{hb} = \left[\frac{C}{d^8} - \frac{D}{d^6} \right] f(\theta, \theta', \ldots)$$

Figure 2. The empirical energy functions used in MCSS and GRID.

which are required by the Slater–Kirkwood formula to determine the A and B parameters of the Lennard–Jones potential function. An aromatic hydroxyl probe is modelled as an oxygen center, whose properties reflect the presence of an attached hydrogen and also an attached benzyl ring. It is characterized like the methane probe, but has two additional parameters, E_{min}(HB) and r_{min}(HB), which are used to determine the C and D parameters of the hydrogen bonding potential function [1] (cf., Figure 2).

GRID hydrogen bonding function

The GRID hydrogen bonding function (HBE) (Figure 2) includes a 8-6 potential which is similar in form to the Lennard–Jones potential. It also has angle dependent terms, the forms of which depend on the particular probe being studied [2–4]. Since the GRID water probe is examined in detail in this paper, the hydrogen bonding properties of this probe will be described (other probes are discussed in [2–4]). The hydrogen positions in the spherical GRID water probe are not specified explicitly, and their most favorable orientation at each probe position is determined as follows. First, it is assumed that one hydrogen bond is linear (along the water O–H bond, the lone pair direction, or the bisector of the lone pairs). This assumption fixes an orientation of the water probe, and thus also a hydrogen bonding coordination geometry, which then is classified as either tetrahedral or triangular (the latter involves one hydrogen bond accepted by water along the bisector of its lone-pair orbitals; these geometries were chosen because they are most commonly seen in crystal structures of biological molecules). The energy of the remaining hydrogen bonds is evaluated using suitable angle-dependent correction terms, which correct for deviations from the selected ideal geometry [4]. This process is repeated by assuming each of the hydrogen bonds in turn to be linear. The combination that results in the lowest overall hydrogen bonding energy for the probe is selected. The GRID water probe is modelled as single neutral sphere with implicit hydrogens (see above); hence the HBE term accounts for almost all of the nonbonded interactions, as there is no electrostatic term and the van der Waals term is usually negligible by comparison. (If the van der Waals contribution is not favorable it is neglected in GRID, which thus does not use the van der Waals repulsive term to delimit the closest approach in a hydrogen bond.) Some of the other polar GRID probes (e.g., the aromatic hydroxyl probe) have small partial charges and thus also have a nonzero electrostatic interaction between the atoms involved in the hydrogen bond, though this always is small compared with the HBE.

MCSS calculations

Functional group minima maps were generated using the standard MCSS method [5, 6]. For poliovirus, 1500 group copies initially were distributed randomly within a $21 \times 19 \times 31$ Å^3 box, centered on the binding site (Figure 1) [13]. For src SH3, the same number of group copies were distributed within a $25 \times 20.5 \times 15$ Å^3 box which nearly encloses the entire protein. In both cases, the group copies are energy minimized simultaneously with the time-dependent Hartree approximation used in the MCSS method [27]. This approximation is exact for a rigid protein, and each group copy feels the full force field of the protein, but the copies do not interact with each other. For each MCSS calculation, the group copies were subjected to 800 steps of steepest descent followed by up to twenty cycles, each of 500 steps, of conjugate gradient minimization. If the root-mean-square gradient falls below a 0.01 kcal/mol Å tolerance, the minimization stops before the specified number of steps. The default gather cutoff distance and energies were used; i.e., after every minimization cycle, the group copies are gathered to remove duplicates: if the rms all-atom difference between two copies is equal to or less than 0.2 Å and the difference has decreased relative to the last cycle, then one of the two copies is deleted. Also, after the second cycle, all copies with energies greater than 250 kcal/mol are eliminated, and this energy cutoff decreases geometrically with each cycle, reaching 3 kcal/mol after 10 iterations (i.e., 250 $\rightarrow$ 126.5 $\rightarrow$ 64.75 $\rightarrow\rightarrow$ 3). In a series of test calculations using methane, it was found that the map obtained using 3000 copies is nearly identical to others in which the copy number is increased (e.g., up to 30 000 copies), indicating that MCSS rapidly and effectively determines the local potential energy mimina. With a higher copy number, occasional higher energy minima are observed in isolated areas within the protein interior, but the distribution of minima within the binding pocket remains the same.

The MCSS energy (Figure 2) includes protein-group nonbonded terms (van der Waals and electrostatic) and intra-group nonbonded and bonded terms minus a vacuum reference energy for the group [13]. The energy thus accounts for the bonded and non-

bonded strain introduced into the group upon binding. The CHARMM PARAM19 [28] and PARAM22 [24] force fields do not include an explicit hydrogen bond term, and have been parametrized to account for hydrogen bonding via the standard electrostatic and van der Waals terms. For charged and polar groups, only minima with energies less than the group solvation energy were examined [13]. For all other groups, minima with energies less than zero were included. In the results that follow, minima are numbered in ascending order based on their interaction energy; i.e., the lowest-energy minimum is labelled #1, the second-lowest #2, etc.

The hybrid hydrogen representation was used for the MCSS calculations [5]. In the hybrid scheme the standard PARAM22 (all-hydrogen) parameters are used for the protein and the standard PARAM19 (polar hydrogen) parameters for the functional group. The energy function minimized by CHARMM used a constant dielectric of unity and the shift function for truncating nonbonded terms, with a nonbond cutoff of 7.5 Å. The shift function is applied from an interaction distance of zero to ctofnb (here 7.5 Å) and beyond ctofnb the interaction term is zero; cutnb (8.5 Å) determines which atoms are included in the list of pairs used for the calculation of nonbonded terms. Unless otherwise noted (see below), the shift function with these parameters was used in all calculations. The MCSS functional group maps examined in this report are methane, water, phenol, cyclohexane, methylpyradizine, and methylpyradizinyl-piperidine (Figure 9). The last two MCSS groups (fragments of the Janssen compound, R78206) were created according to standard procedures [5, 6]. Atomic partial charges were determined using MMFF [29].

In the results section for the water group, the hydrogen bonding energy of MCSS water is estimated to compare it with the GRID results. This estimate is made as follows. The nonbonded (van der Waals and electrostatic) interactions are summed for only those atoms involved in the hydrogen bond. For protein acceptors, nonbonded terms for the protein acceptor atom interacting with the three water atoms are included; for protein donors, terms for the protein heavy atom and also for its hydrogen interacting with the three water atoms are included. In some cases both hydrogens bonded to the protein donor appear to be involved in the hydrogen bond and hence both are included; e.g., when the guanidinium nitrogen of arginine donates, both of its hydrogens are included in the calculation if a 'bridging' interaction with the water oxygen is observed. This estimate of the MCSS HBE completely describes the nonbonded interactions between the four or more atoms (three water atoms plus one or more protein atoms) involved in the hydrogen bond and thus can be compared to the GRID HBE (see below). It should be noted that the MCSS HBE estimate given here considers the electrostatic interactions of the water group with isolated protein atoms rather than with neutral protein units (e.g., for a hydrogen bond to a carbonyl oxygen, only the interaction with the partially-charged oxygen is considered, though this oxygen is part of a carbonyl unit which is neutral overall). This limitation is not expected to affect its usefulness as a relative measure of the hydrogen bonding energy which can be compared with the GRID results.

As a test of the sensitivity of the results to the cutoff of the energy function, an MCSS methane map was calculated using the switch truncation function, where the switching function is introduced at 6.5 Å and goes to zero at 7.5 Å. (All pairs within 8.5 Å are included in the nonbonded list; see [26] for details.) The positions and energies of the methane minima determined using the switch function and the shift function are nearly identical. As a further test, the methane minima determined using the shift function were reexamined in a post-processing step by recalculating the energy: (i) according to a truncation scheme without a smoothing function, in which all interactions beyond 7.5 Å were ignored; and (ii) according to the switch truncation function with the cutoffs listed above. Method (i) was carried out using the CHARMM COOR DIST command, which calculates nonbonded pairwise interactions between group atoms and protein atoms; all interactions within 7.5 Å were summed to give the interaction energy. (This is reasonable only for nonpolar groups, however, since electrostatic interactions are still significant at 7.5 Å, and therefore should not simply be truncated.) Note that the shift truncation function is applied over the entire range of interaction and works by shifting the nonbonded energy curves upward, thus exaggerating any van der Waals repulsion between two atoms with overlapping van der Waals radii. Methods (i) and (ii) avoid this difficulty.

The MCSS functional groups are modelled using the polar hydrogen (PARAM19) representation, in which all heavy atoms and polar hydrogens are represented explicitly, and nonpolar hydrogens are united with the heavy atom to which they are attached. Consequently, while a methane functional group consists of a single sphere, all other functional groups have

multiple centers; for example, the phenol group consists of eight explicit centers (six aromatic carbons, an oxygen, and a hydrogen). The standard CHARMM nonbunded parameters (i.e., minimum radius and epsilon values, and partial atomic charges), as well as the parameters relevant to internal (bonded) terms, were used; these are described in Neria et al. (1996) for PARAM19 and in MacKerell et al. (1998) for PARAM22.

Analysis

Several methods of comparison were used in this study. First, for like functional groups, correspondence was assessed visually by comparing the distribution of MCSS minima with a GRID contour map, which is used to identify relative minima. This comparison is based on the fact that GRID results have been used this way in published examples; e.g., in the improvement of a neuraminidase inhibitor [10]. In this example, maps for several probes were contoured. The amino probe map identified a relative minimum overlapping the position of a hydroxyl group of the inhibitor in the crystal structure complex. Since the hydroxyl probe map did not indicate a relative minimum at or near this position, the amino group (and eventually a guanidinyl group) was substituted. Similarly, water positions have been identified for comparison with crystal waters by determining the relative minima of a contour map for the water probe.

In the second method of comparison, the GRID probe energy was evaluated at the positions of the MCSS minima for each functional group. This permits a direct comparison of the empirical energy functions used by the two methods. Correlation statistics were calculated to compare a set of MCSS minima energies with the corresponding set of GRID energies determined at the MCSS minima. A correlation coefficient (MCSS : GRID) was calculated. It is defined as the covariance of the energy values divided by the product of their standard deviations; i.e.

$$\frac{\langle (E_{MCSS} - \bar{E}_{MCSS})\,(E_{GRID} - \bar{E}_{GRID}) \rangle}{\sqrt{\frac{1}{N}\sum_{i=1}^{N} (E_{MCSS} - \bar{E}_{MCSS})^2}\sqrt{\frac{1}{N}\sum_{i=1}^{N} (E_{GRID} - \bar{E}_{GRID})^2}}.$$

These two approaches were used to compare methane, water, phenol, and cyclohexane groups for the poliovirus capsid protein and to some extent for the src SH3 domain. For the water probe, the hydrogen bonding geometries and the contributions of hydrogen bonding to the total interaction energies were examined for selected cases. For the phenol group, a few MCSS minima in different regions of the poliovirus binding site were examined and the contributions of different components to the total interaction energy were determined. Finally, the ability of the two methods to find the crystallographically observed positions of ligand moieties was examined; specifically, the optimal locations of fragments of the antiviral drug R78206 were determined using both methods and these results were compared to the crystal structure of the complex.

Table 1. Computational timings[a] for MCSS and GRID calculations

Probe type	MCSS[b]	GRID[c]
Methane	58.9	13.6
Water	111.5	14.0
Methanol	103.2	19.5
Phenol/aromatic OH	261.0	19.6

[a]Times are given in CPU minutes.
[b]A 1500 copy MCSS search was performed in each case.
[c]The GRID search box exceeds the MCSS placement box by 2 Å in each dimension.

CPU timings are given for calculations on a single SGI R5000 processor. Table 1 compares the CPU time for selected functional groups, and indicates that though the GRID method is faster, neither method is prohibitive. In considering these results, it is important to note that, for example, the MCSS phenol group (in the polar hydrogen representation) involves eight explicit atoms, while the corresponding GRID aromatic hydroxyl probe involves only a single sphere that approximates the hydroxyl moiety; the presence of the aromatic ring is neglected. However, even in the case of methane, where both methods use a single-sphere probe, GRID is faster; this is the result of its grid-based approach, which corresponds to a zeroth-order approximation to finding minima. MCSS is more time-consuming in part because it is a first-order approach; i.e., it calculates the derivatives of the potential energy in order to find minima.

Results

Methane

The methane probe has been used in applications of both MCSS and GRID to identify hydrophobic regions in an area of interest [6, 9, 10]. Methane permits the

most direct comparison of the MCSS and GRID functional group maps and their corresponding van der Waals energy functions. This is true because, in the PARAM19 representation, the MCSS methane group is modelled as an extended carbon atom; i.e., it is represented as a single sphere with no internal interactions, as are the GRID probes. By contrast, the remaining MCSS groups all involve multiple heavy atoms and/or polar hydrogens, all of which are represented explicitly. Thus, the MCSS groups are essentially different from the single sphere model used in GRID.

An MCSS methane map was determined for the poliovirus binding site (Figure 3). There were 46 minima using the standard cutoff criteria (see Methods), and they ranged from −4.24 kcal/mol to −0.04 kcal/mol. The GRID methane map calculated for the binding site box indicates many energetically favorable positions. Since GRID does not calculate minima, these results usually are displayed as contour maps. Figure 3 shows the GRID results contoured at various energy levels and the positions of the MCSS minima. Contouring at successively lower energies isolates peaks which correspond to local minima on the GRID energy surface. Inspection of Figure 3 indicates that most of the MCSS minima lie within or near the GRID density peaks. In the binding pocket, MCSS minima also overlap well with the crystallographic positions of the methylene carbons of sphingosine; six of the first eleven carbons starting deepest in the binding pocket (i.e. from the top of the figure) have a MCSS methane minimum within 1.1 Å. Figure 3C indicates that four of these MCSS minima are within the GRID density contoured at −3.5 kcal/mol; the remaining two also are enclosed at a slightly higher energy contour (−3.30 kcal/mol).

Figure 4 indicates that for methane there is an approximately linear relation between the energies of most MCSS minima and of the GRID probe evaluated at the identical positions, using the same nonbond cutoff distance (1.5 Å). For some of the higher energy MCSS minima (#40, 43–46, in the range −2.11 to −0.04 kcal/mole), however, the corresponding GRID energies are anomalously lower. These deviations result from a difference in the van der Waals radii of the two probes; the GRID probe is slightly smaller (1.95 Å) than the MCSS group (2.09 Å) and therefore has a very favorable energy at positions that are so close to the protein that the larger MCSS group experiences a significant van der Waals repulsion. However, these positions are located in isolated regions of the GRID contour map and are not near the relevant area for ligand binding. Unlike the shift truncation, the switch function does not modify close-range interactions (see Methods). Using the latter to calculate the MCSS energy lessens the energy difference at these sites. If these five sites are excluded, the correlation between the two energy sets is 0.955. A methane MCSS map for the src SH3 domain indicates 62 minima, ranging from −3.58 kcal/mol to −0.24 kcal/mol. These minima are distributed broadly across the surface of the domain and, again, they lie mostly within or near the GRID density peaks. A linear relation also is observed when the GRID probe is evaluated as before at these positions; neglecting the highest energy minimum (again because of the van der Waals repulsion), the correlation is 0.964. The MCSS and GRID calculations for both systems are done in vacuum. One advantage of MCSS is that solvent can be included implicitly using recently developed solvent models, such as EEF1 or ACE, which are part of the CHARMM program suite. GRID accounts for solvent approximately in its calculation of electrostatic interactions, which are nonexistent in this case; in the case of polar probes, they are much less significant than the hydrogen bond interactions (see below).

The methane functional group involves only van der Waals interactions with the target structure, and MCSS and GRID both evaluate this term using a 6–12 Lennard–Jones potential. Thus, the good agreement in the energy values was expected. The GRID energy values, however, are systematically larger by about 15%. Both the truncation scheme used by MCSS and differences in the nonbonded parameter values appear to contribute to this effect. Thus, while the MCSS energies remain smaller when recalculated using the switch function, if MCSS methane is evaluated using no cutoff function (which is identical to what is done in the standard GRID calculation), then the energy values are systematically larger than the GRID values ($R = 0.949$). Hence the truncation scheme used affects the magnitude of the MCSS energies, but not their correlation with the corresponding GRID energies. For most protein atom types interacting with the methane probe, the nonbonded parameter values (e.g., the well depths of the van der Waals interaction term [ε_{ij}]) are quite similar. However, there are subtle differences which are not amenable to any simple rule. Table 2 gives the ε_{ii} values for various GRID probes and the corresponding CHARMM atom types as examples. There also are slight differences in the r_{min} values used by the two methods. In sum, there are minor differences

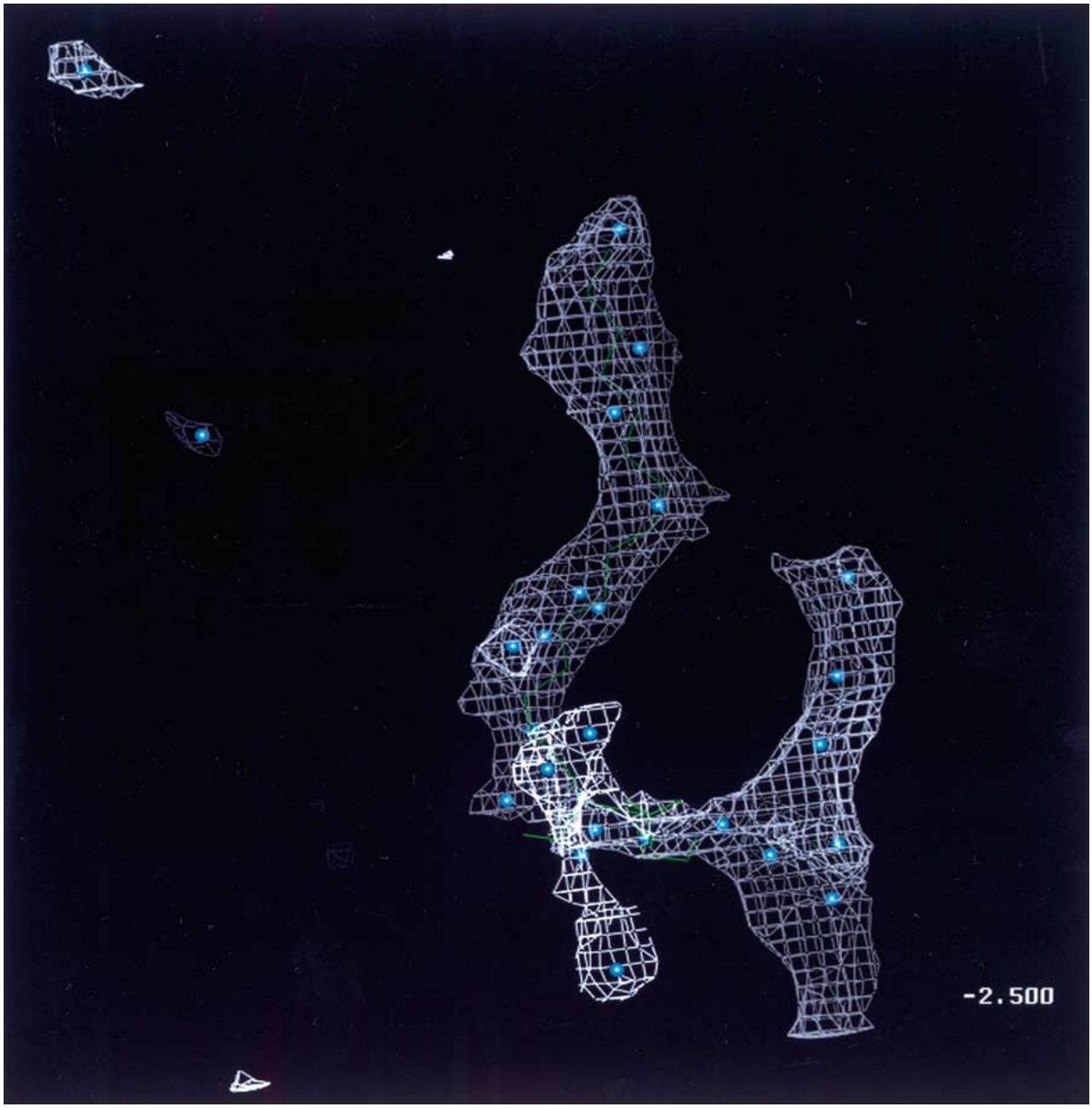

Figure 3a. A comparison of MCSS methane minima and the corresponding GRID map for the poliovirus structure, contoured at (a) −2.5 kcal/mol, (b) −3.0 kcal/mol, and (c) −3.5 kcal/mol. A map contoured at, e.g., −2.5 kcal/mol means that all grid points with energies less than or equal to −2.5 kcal/mol are shown. Adjacent grid points satisfying this criterion are connected, and thus form lobes of density similar to those found in an electron density map. The MCSS minima with an energy less than zero are shown as small blue spheres in each of the three figures. Due to the view chosen, not all MCSS minima are visible in these pictures. (Note that for all probes, a GRID map contoured at about −2.0 kcal/mol outlines the van der Waals surface of the binding pocket.)

in the nonbonded parameter values which contribute to the difference in the energy values. Insofar as these differences in energy values are regular and independent of the method (or absence) of cutoff, they do not affect the *relative* energies, of the minima, nor the distribution of the minima within the binding site. The results for methane are a model for the van der Waals interactions between a functional group and the protein, and indicate that the two methods compare well in this respect.

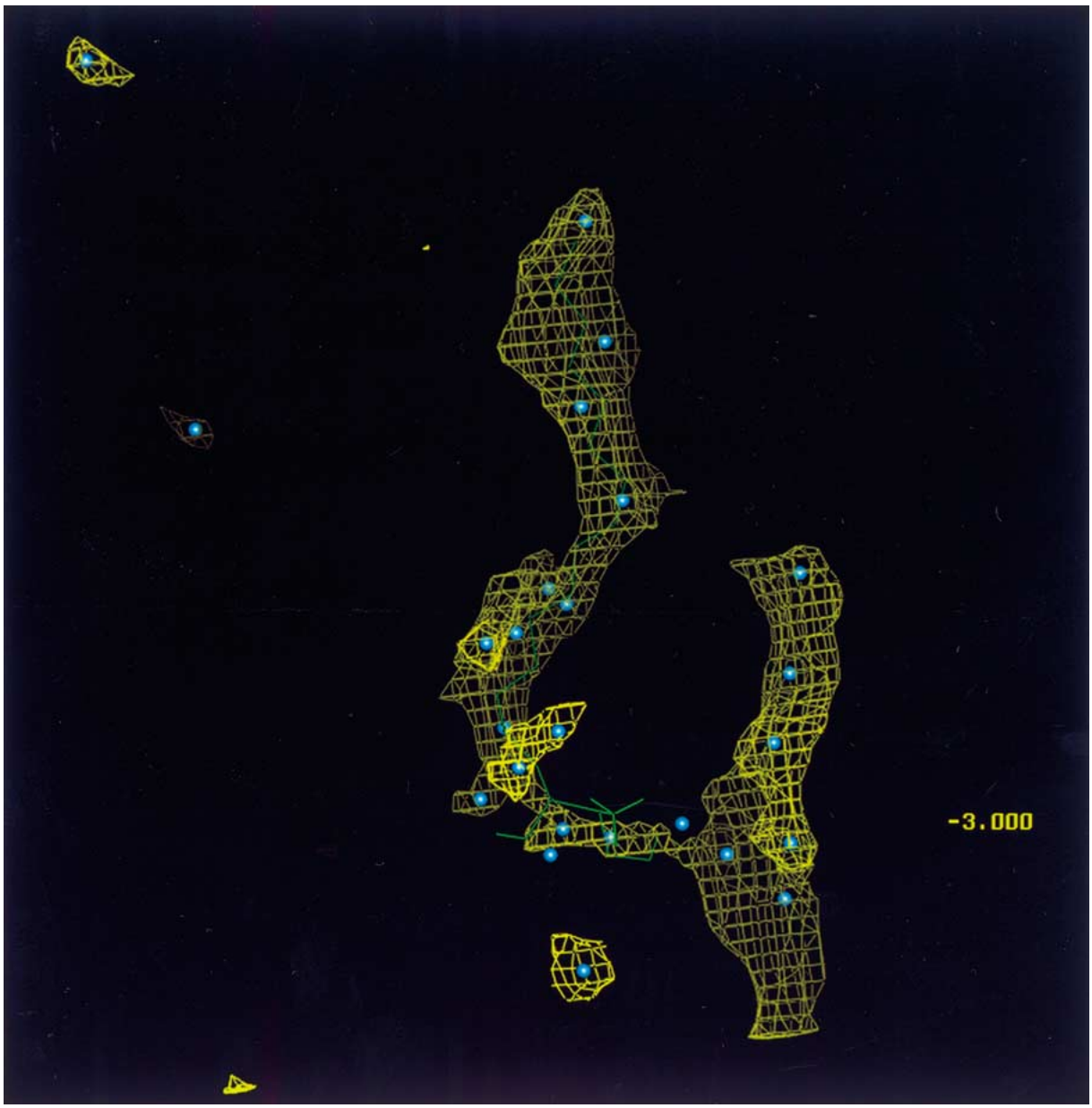

Figure 3b. (Continued.)

Water

The water group is the smallest polar MCSS group and can be considered a model of protein-group polar interactions, for which the functional form of the MCSS and GRID energy functions differs (cf., Figure 2). The water group might be used, for example, to search for or corroborate the position of a conserved water important to an enzymatic reaction; to aid in the placement of crystallographic waters, particularly internal waters and those of the first hydration shell; or to suggest where a lead compound might be functionalized with a hydroxyl or other oxygen-containing polar group. The GRID method treats the interactions of water with the protein as a sum of hydrogen bonding and van der Waals terms for the sphere representing the water placed at each GRID point (see Methods). In contrast, the MCSS interaction energy for water includes electrostatic interactions with protein atoms

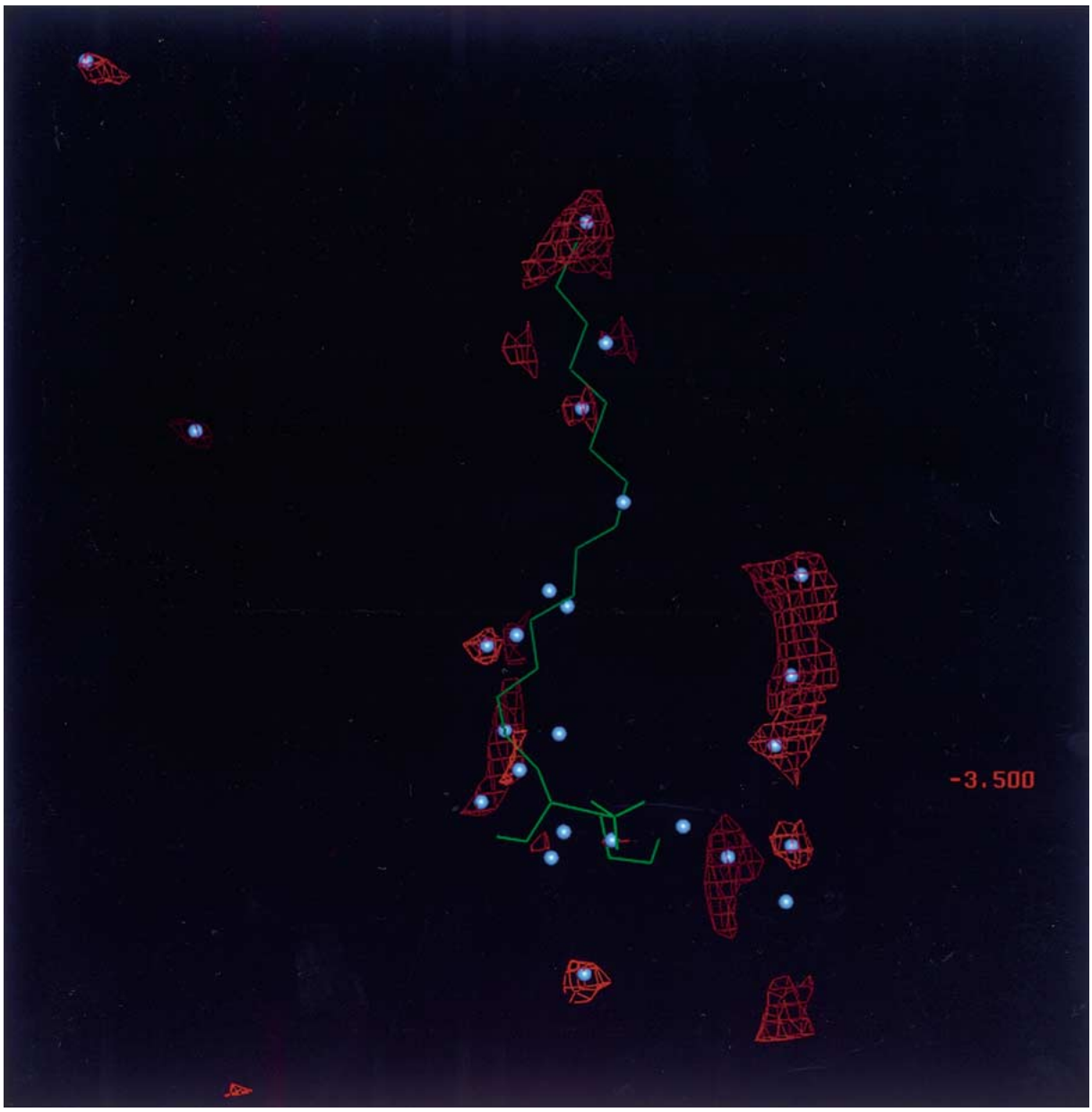

Figure 3c. (Continued.)

beyond those specifically engaged in hydrogen bonding. This is because the MCSS water group (TIP3P model) represents all three atoms explicitly and each partially-charged atom of an MCSS water interacts with the charges of all protein atoms within the nonbond cutoff. The hydrogen bond arises primarily from the electrostatic term in the potential energy function, while the angular range and closest approach are determined by the van der Waals term. In contrast to GRID, MCSS minimization places no *a priori* restrictions on the hydrogen bonding geometry. Also, the MCSS interaction energy generally includes internal terms, but these do not contribute in this case, since water has a rigid geometry in the TIP3P model.

Despite these differences in how polar interactions are defined and calculated, the MCSS distribution of minima and the GRID water maps are qualitatively similar (Figure 5). The MCSS water map for po-

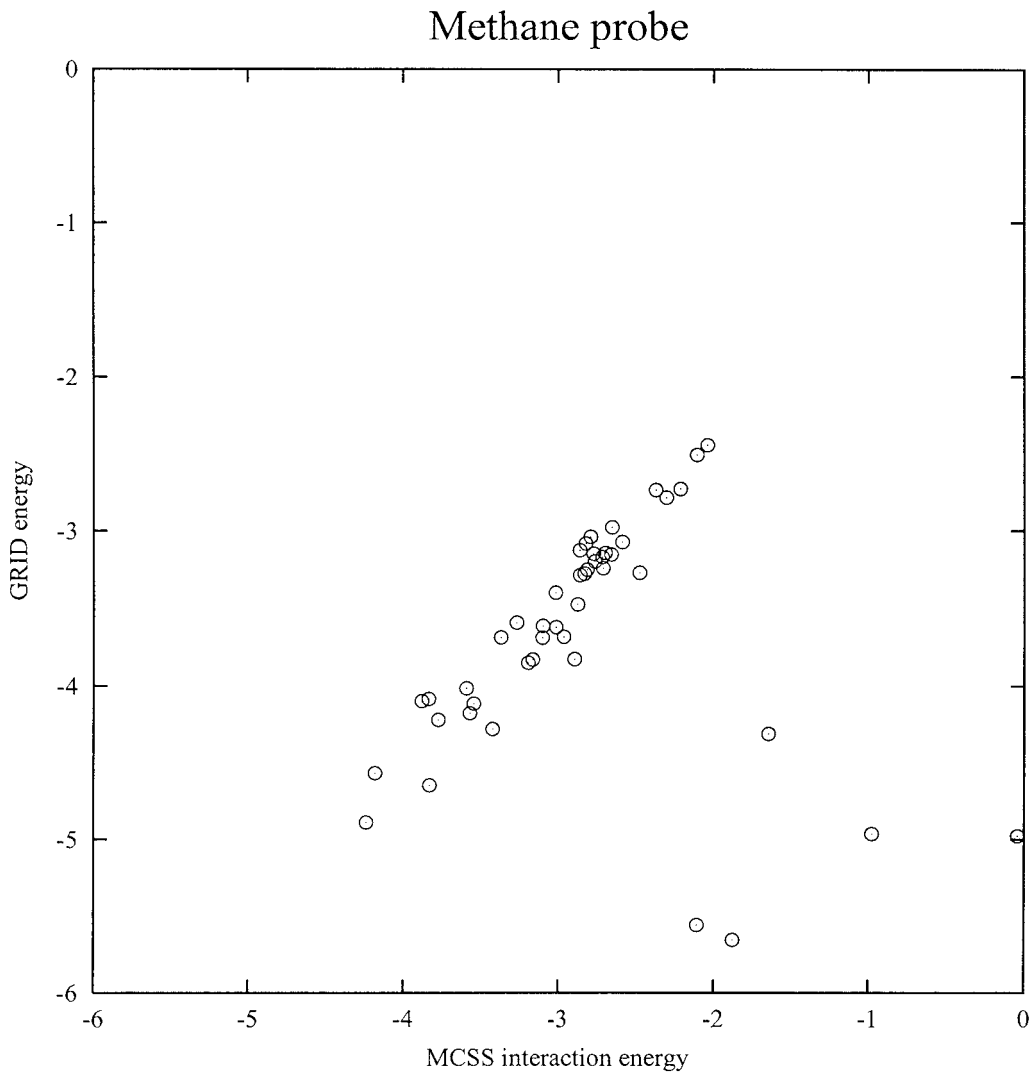

Figure 4. Interaction energies of MCSS methane minima with the poliovirus capsid protein versus the GRID methane probe energy evaluated at the same positions (see text for details).

liovirus consists of 97 minima with energies less than the solvation free energy of water (−5.0 kcal/mol), which is the cutoff used in Figure 5; the lowest energy minimum is −41.57 kcal/mol. The GRID energies are substantially less negative: within the grid search box, the lowest energy point is −16.22 kcal/mol. Many MCSS water minima lie within or near the peaks of GRID density (cf., Figure 5). The MCSS water minima that do not fall within the GRID density shown in Figure 5 have relatively higher energies (in the range −7.0 to −5.0 kcal/mol), and thus would fall within higher energy GRID contours (not shown). Also, characteristically, these minima are found mostly in the buried, upper portion of the binding pocket (cf., phenol results, below). In contrast to methane, a consistent ratio was not observed between the energies of the MCSS minima and of the GRID probe evaluated at the same positions. However, MCSS minima often are observed to cluster in groups of two or more, and Table 3 lists the clusters observed in the MCSS water map. When the ratio of MCSS:GRID energies is compared only for positions within the same cluster, the magnitude is similar (Table 3). This is important because in both MCSS and GRID, it is the local minimum within a particular small region that is relevant to drug design, and these results indicate that within such small regions (defined here by the clusters) the two methods correspond. Between clusters, however,

Table 2. Parameters for GRID probes vs. MCSS atom types

Probe/atom type	Well depth (ε_{ii}) (kcal/mol)	Minimum radius (Å)
Methane / CH4	−0.232 / −0.294	1.95 / 2.09
Water / OT	−0.203 / −0.152	1.70 / 1.77
Aromatic OH / OH1	−0.341 / −0.159	1.65 / 1.60
sp^2 nitrogen / NR	−0.414 / −0.238	1.65 / 1.60

The well depth ε_{ii} refers to the minimum energy of the van der Waals curve describing the interaction of two identical probes. The well depth for the interaction of a probe with a protein atom is determined by taking the geometric mean of the ε_{ii} values. The GRID parameters include the polarizability and the number of effective electrons, from which the parameter B (cf. Figure 2) is determined via the Slater–Kirkwood formula. Using B and r_{min}, parameter A as well as ε can be calculated from the Lennard–Jones equation. The ε_{ii} values listed here for GRID probes were calculated using the standard GRID parameters. The GRID sp^2 nitrogen probe is neutral with a lone-pair. The MCSS atom types CH4, OT, OH1 and NR, correspond respectively to a methane carbon, TIP3P water oxygen, hydroxyl oxygen, and a nitrogen in an aromatic ring with no hydrogens.

the magnitude varies irregularly, reflecting differences in the form of the potential energy function and in the determination of geometry. This is distinct from the case of methane, for which the energies differed in a regular manner.

In MCSS and GRID, electrostatic and hydrogen bonding contributions, respectively, dominate the energy of the most favorable water positions. For example, in GRID, the water map contoured at −2.0 kcal/mol traces the van der Waals surface, i.e., like the methane map at this contour it outlines the binding pocket and all other accessible surfaces of the cutout region of the protein. The water map contoured at −4.5 kcal/mol (Figure 5, yellow) does not. Instead, such lower energy GRID contours for polar probes, such as water, nearly always involve hydrogen bonding interactions.

Hydrogen bonding patterns were examined for the five lowest energy MCSS minima clusters (cf., Table 3) and for nearby low-energy points identified by GRID. The orientation assumed by water at each position was compared. Since GRID probes lack explicit hydrogens, the hydrogen positions must be inferred from the set of allowed reference geometries and from the hydrogen bonds selected for inclusion in the energy calculation (see Methods). The results for the two methods generally were rather similar. MCSS water minima #2 and #12 (cluster 1 listed in Table 3) both donate a hydrogen bond to Glu 1133 OE1 and accept from Lys 1265 NZ-HZ1. In addition, #2 donates to His 3019 O, while #12 donates to Ser 1195 OG. The lowest energy nearby GRID point is located 0.31 Å and 0.28 Å from the oxygens of #2 and #12, respectively, and has the same hydrogen bonding network as #12, while another low-energy nearby GRID point has the same network as #2. In cluster 3 listed in Table 3, MCSS minima #7 and #9 share the same hydrogen bonding network: both donate to Glu 1123 OE2 and accept from Lys 1113 NZ-HZ3 and Tyr 1112 OH. The lowest energy nearby GRID point is 1.57 Å and 0.56 Å from the oxygens of #7 and #9, respectively and has the same hydrogen bonding network. A slightly higher energy GRID point has the Glu, His, and Lys hydrogen bonds but lacks the Tyr hydrogen bond. Minima #8, #10 and #11 (cluster 4) again share the same hydrogen bonding network, donating to Asp 1237 OD1 and accepting from Lys 1113 NZ-HZ2. The two nearby low-energy GRID points also make these hydrogen

Table 3. Ratio of MCSS and GRID interaction energies by cluster

Cluster No.[a]	MCSS minima[b]	Ratio of MCSS energy: GRID energy[c]
1	2, 12	5.5, 4.4
2	3, 5, 6	4.6, 3.4, 4.2
3	7, 9	2.5, 3.1
4	8, 10, 11	5.2, 5.4, 5.6
5	16, 21	4.3, 4.2
6	29, 34, 44	1.7, 2.3, 2.4
7	43, 50	1.5, 1.0
8	45, 52, 53, 54, 55, 58	2.0, 1.6, 1.4, 1.3, 1.8, 1.0
9	56, 65	1.1, 1.0
10	60, 62, 64	1.5, 1.4, 1.6
11	68, 70, 71, 72, 92, 94	2.5, 3.6, 3.7, 2.8, 2.8, 2.6
13	73, 74	2.5, 2.2
14	79, 80	2.4, 2.3
15	81, 82	2.6, 2.8
16	83, 86	0.6, 0.5
17	84, 85	2.7, 2.6
18	87, 90	0.7, 1.1
19	75, 89, 91	1.0, 0.8, 0.8
20	96, 97	1.1, 1.3

[a]Clusters were determined by visual inspection of the MCSS water minima map. About one half of the minima were segregated into clusters; the remaining 'lone' minima usually were outside of the binding pocket.
[b]The number of each minimum in the cluster. The minima are numbered starting 'in ascending order' with the lowest energy one.
[c]Ratio of MCSS interaction energy to the GRID energy calculated at the MCSS minimum position.

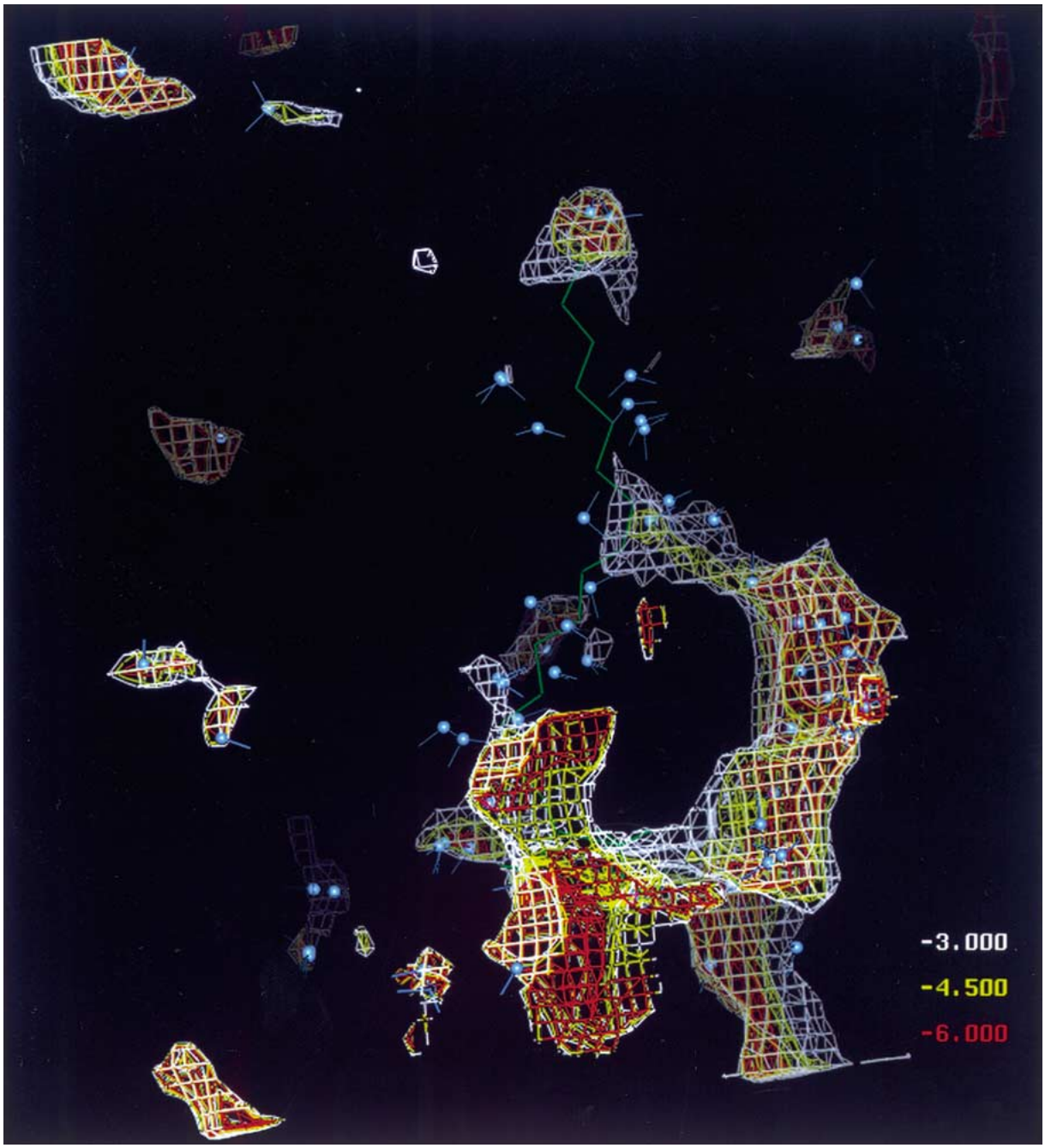

Figure 5. A comparison of MCSS water minima and the corresponding GRID map for the poliovirus structure, contoured as indicated (all contour levels given here and in subsequent figures are in kcal/mol). The MCSS minima with energies less than −5.0 kcal/mol (the solvation energy of water) are shown in a ball-and-stick representation, with the oxygens as blue spheres.

bonds and each makes an additional (weaker) hydrogen bond, one to an arginine NH1, the other to a serine O. Minima #16 and #21 (cluster 5) share the same hydrogen bonding network: both donate to Asp 1237 OD2 and accept from Thr 1234 N. The three nearby low-energy GRID points have the same network. This analysis indicates that the GRID hydrogen bonding function results in hydrogen bonding patterns similar to those achieved by MCSS, and thus also orients the GRID water hydrogens analogously. This is consistent with the qualitative agreement observed between the MCSS and GRID maps.

For cluster 2, comprising minima #3–6, a more detailed analysis was made, i.e., GRID probes were placed at exactly the positions of the MCSS minima and examined. MCSS minima #3–6 share three common hydrogen bonds (Figure 6), one with Arg 2140 NH1 as the donor, another with Asp 1237 OD1 as the acceptor, and a third with Thr 1234 O as the acceptor. #4 and #5 make an additional hydrogen bond with Met 1233 N as the donor. Consistently, at the positions of #3 and #6, GRID specifies a triangular reference geometry for the same three hydrogen bonds. The two hydrogen bonds donated by the probe are compared to ideal tetrahedral positions (established by setting the stronger hydrogen bond to be linear) and the one accepted hydrogen bond is compared to the bisector of the lone-pair orbitals of the probe [4] (cf., Methods). At the positions of minima 4 and 5, GRID selects a tetrahedral reference geometry. In this case, the four hydrogen bonds identified are compared to ideal tetrahedral positions, again set by requiring the lowest energy hydrogen bond to be linear. Table 4 summarizes the energetics of MCSS minima #3–6 and of the GRID probes at the same positions. It is seen that while the magnitudes of the TE and HBE differ between the two methods, the HBE/TE ratio is similar for both. Indeed, in general, this ratio is fairly regular in GRID: its average over all of the nearby, low-energy GRID points examined in the first five clusters is 0.78 ($N = 11$, range: 0.70–0.86) (in the case of water, the remainder of the total energy is due to van der Waals contributions). This reflects the dominance of hydrogen bonding contributions to the total GRID energy in the case of polar probes such as water. Notably, the MCSS estimate reproduces this ratio, making it useful for purposes of comparison.

To illustrate the problems that can arise from the specific hydrogen bonding function in GRID for a relatively strongly bound water, we consider MCSS minimum #25 (Table 4; not listed in Table 3 because it is not part of a cluster). This MCSS minimum was selected for analysis because its total interaction energy differs greatly from that of the GRID cognate. The MCSS minimum has a HBE/TE ratio of 0.77, which is consistent with the other MCSS and GRID cases in Table 4 and elsewhere, but the HBE/TE ratio of the GRID cognate is 2.13, which is irregular. MCSS minimum #25 accepts two hydrogen bonds from protein donors, and donates to a very close Asp 1131 OD1; the hydrogen-oxygen distance is 1.62 Å. At the same position, the GRID probe accepts the two hydrogen bonds, but fails to donate to Asp 1131 OD1 and thus its corresponding (repulsive) van der Waals interaction (+6.43 kcal/mol) with this atom is retained. Thus the HBE is, inconsistently, much lower than TE.

Three nearby low-energy GRID points are included in Table 4. At each site, the GRID probe donates a hydrogen bond to Asp 1131 OD1, while maintaining the other two hydrogen bonds. This new hydrogen bonding interaction with Asp 1131 OD1 requires that the repulsive van der Waals interaction be neglected (cf., Methods). The total GRID interaction energy improves by about ten kcal/mol, the HBE improves correspondingly, and the HBE/TE ratio (0.78, 0.73, 0.66) is consistent with the other results. Though the GRID probe at the position of MCSS minimum #25 is very close to these other three points, it fails to hydrogen bond with Asp 1131 OD1 due to imposed tetrahedral geometry constraints which enforce a very acute angle between the Asp 1131 OD1 and the relevant water hydrogen. That is, the hydrogen bonding algorithm compels the probe to select either the two protein donors alone or the one acceptor alone and, since the two protein donors are preferred energetically over the one acceptor, the former geometry prevails, requiring inclusion of the van der Waals repulsion term associated with Asp 1131 OD1. Although no MCSS water minima were found at these three additional points, the MCSS energy was evaluated for the water group with its oxygen fixed at the three positions. (Note that this is the inverse of the earlier procedure, e.g., Table 3, in which the GRID probe is set at the locations of the MCSS minima.) The optimal orientation of each water was determined by minimizing the orientation while keeping the oxygen position fixed; in each case, the hydrogen bonding network is consistent. At these sites, the MCSS energy and HBE is consistent with that of minimum #25 and other minima (Table 4). This example illustrates an effect of using a functional form for the interaction (such as MCSS) which includes hydrogen bonding

Table 4. Hydrogen bonding of the water probe

MCSS	MCSS			GRID			TE_{MCSS}/
	HBE[a]	TE	HBE/TE	HBE[a]	TE	HBE/TE	TE_{GRID}
3	−28.16	−34.92	0.81	−6.28	−7.66	0.82	4.26
4	−28.27	−34.86	0.81	−11.83	−14.31	0.83	2.43
5	−29.18	−34.70	0.84	−8.22	−10.30	0.82	3.31
6	−23.50	−34.67	0.68	6.87	−8.35	0.82	4.12
23	−19.60	−25.05	0.78	−0.43	−1.16	0.37	21.59
25	−18.48	−23.23	0.77	−4.70	−2.21	2.13.	10.82
25-case1[b]	−15.80	−20.00	0.79	−9.48	−12.15	0.78	1.65
25-case2[b]	−19.52	−26.83	0.73	−10.06	−13.81	0.73	1.94
25-case3[b]	−21.68	−24.14	0.90	−7.62	−11.50	0.66	2.10

[a]HBE = hydrogen bonding energy; TE = total interaction energy; all energies are given in kcal/mol.
[b]Cases 1–3 are associated with minimum 25 and are nearby, low energy GRID points identified in the GRID output. The rms differences between the position of minimum #25 and cases 1, 2, and 3 are 1.11 Å, 0.43 Å, and 1.93 Å, respectively.

implicitly versus a functional form (such as GRID) which accounts for hydrogen bonding via an explicit, directional term. In the latter, changing the probe position slightly can substantially affect the HBE and TE. For minimum #23 (Table 4), the total MCSS and GRID energies also are very different and the geometric requirements of the hydrogen bonding algorithm are again responsible for the discrepancy. MCSS indicates a strong hydrogen bond donated by water to Asp 1236 OD2 and a much weaker bond accepted from Arg 1109 NH1; the HBE/TE ratio is 0.78 for this minimum. At the same position, GRID reports the second hydrogen bond, but excludes the first. Consequently, the HBE/TE ratio (equal to 0.37) is very low. As in the case of minimum #25, however, at other positions near #23, GRID makes both hydrogen bonds and its HBE/TE ratio (e.g., 0.73) is within the normal range.

The GRID water probe is parametrized as neutral, which assumes that the electrostatic contributions of the two hydrogens *exactly* cancel those of oxygen, leaving only the hydrogen bonding function to account effectively for charge interactions in the system. In some cases, such as the cluster of minima #3–6, this assumption is adequate, while in others, such as minima 23 and 25, it appears that the directional requirements of the hydrogen bonding function are overly restrictive. In contrast, in MCSS, hydrogen bonding is accounted for primarily via the electrostatic term. Since the two explicit hydrogens and oxygen of an MCSS water have partial charges, their electrostatic interactions with protein atoms usually do not cancel each other (as formally happens in the case of GRID water, since it is neutral). In this way, hydrogen bonding can be accounted for successfully in the MCSS method without introducing cumbersome directional restrictions.

The MCSS water map for the surface of the src SH3 domain has 92 minima, ranging from −33.28 to −1.23 kcal/mol. A good qualitative agreement is observed with the GRID contour map, i.e., the water minima generally lie within or near the GRID density peaks. Again, however, the GRID energies are substantially smaller (the lowest energy point is −12.64 kcal/mol). Thus the results for the src SH3 domain qualitatively confirm those for the poliovirus binding site. Again both calculations are done in vacuum. It is instructive to compare the results of the methane and water probes for this system. The MCSS results show that a methane minimum quite often falls near a water minimum (e.g., within 1–1.5 Å); this is consistent with the larger ε_{ij} values for methane with the type of polar protein atoms with which water interacts favorably. However, there are many additional water minima which are clustered around surface hydrophilic groups, and additional methane minima uniquely clustered around relatively hydrophobic regions of the surface. The GRID results also pick up these effects, though in a less precise way.

Phenol and its hydroxyl moiety

In this section, the MCSS phenol group is compared with the GRID aromatic hydroxyl probe. The phenol group and other rings with attached heteroatoms are particularly relevant for drug design. For example, in

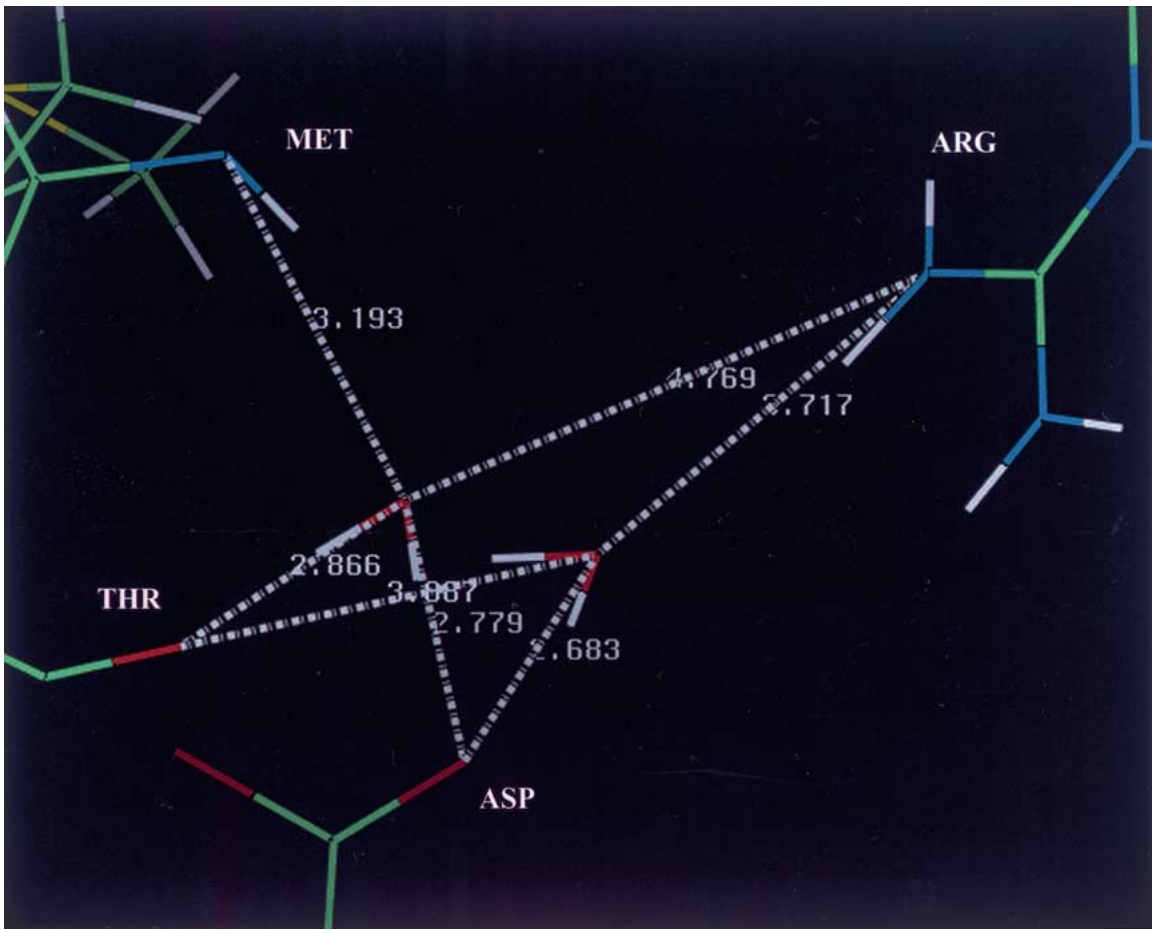

Figure 6. MCSS water minima #3 and #4 shown with the poliovirus capsid protein atoms with which they hydrogen bond according to GRID, namely, ARG 2140 NH1 (upper right corner), ASP 1237 OD1 (lower center), THR 1234 O (lower left corner) and MET 1233 N (upper left corner). Minimum #3 hydrogen bonds only with the first three, and does so with a triangular coordination geometry, while minimum #4 hydrogen bonds with all four using a tetrahedral coordination geometry. (The GRID hydrogen bonding function permits the user to specify the maximum allowed distance for a hydrogen bond, which here was set to the default value, 5.0 Å.)

Joseph-McCarthy et al. (1997), an MCSS phenol map suggested that the binding pocket in the P3/Sabin poliovirus capsid protein could be filled by a bicyclic group connected by a linker carbon to a single ring, connected to another bicyclic group. Further, it was shown that a phenol at the central position could hydrogen bond to Met 1132 of the capsid protein. In the present study, the distribution of MCSS phenol minima was calculated using the hybrid representation and compared to the GRID map for the aromatic hydroxyl probe (cf., Methods). The latter probe does not include a van der Waals radius for the benzene ring; the phenol is represented as an oxygen atom whose partial charge is increased (relative to an aliphatic hydroxyl probe) because it is attached to a benzene ring.

The results are shown in Figure 7, which includes all MCSS phenol minima with an energy less than −12.95 kcal/mol and all GRID points with an energy less than −3.8 kcal/mol. At this GRID contour level, most of the MCSS phenol minima are encompassed within the GRID density, while regions lacking MCSS minima are not filled by GRID density. In some cases, however, the low-energy areas indicated by the GRID single sphere probe are sterically inaccessible to the more realistic MCSS phenol group. The MCSS map has three clusters of phenol minima which span the main binding pocket, and are indicated by arrows. For the cluster deepest in the pocket, the lowest energy minimum (#51, −15.22 kcal/mol) has its hydroxyl group within GRID density; this also is true for the third cluster, where minimum #50 (E =

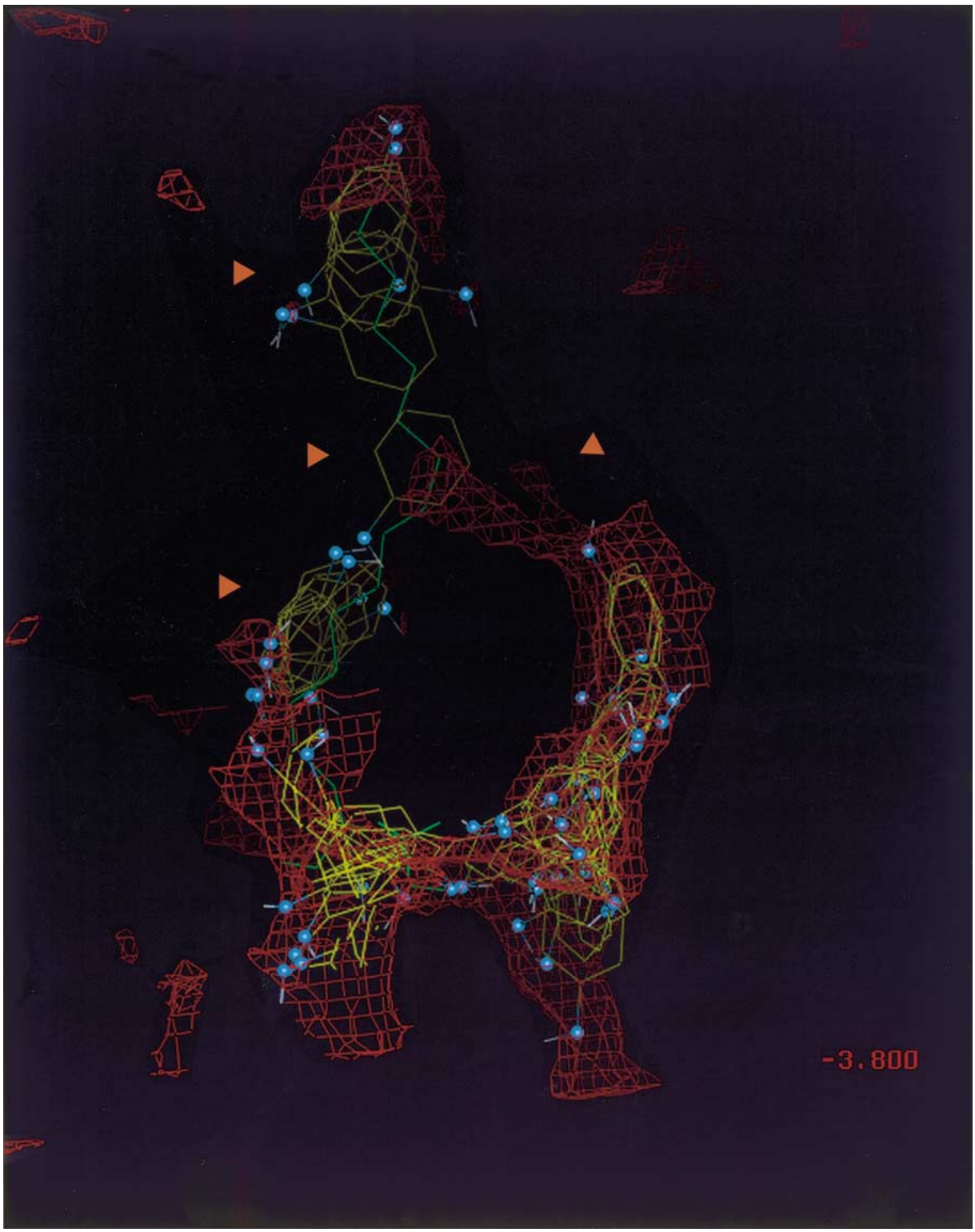

Figure 7. A comparison of the MCSS phenol minima for the poliovirus structure and the corresponding GRID map for an aromatic hydroxyl probe, contoured as indicated. The MCSS minima with an energy less than −12.95 kcal/mol are shown; blue dots indicate the oxygen atoms of these phenol minima. The three triangles on the left point to the three distinct clusters of phenol minima seen in the binding pocket; the triangle on the right points to a lobe of GRID density where the MCSS group is sterically forbidden.

−15.26 kcal/mol) has its hydroxyl within GRID density. At the center of the binding pocket, there is only one phenol minimum (#76, E = −12.98 kcal/mol), and its hydroxyl falls within GRID density when the GRID map is contoured at a somewhat higher energy (−3.0 kcal/mol). There is a large lobe of GRID density in the center of the pocket (right arrow in Figure 7) where no MCSS minimum places the hydroxyl group. A benzene ring attached to a hydroxyl at this position cannot be accommodated sterically in the binding pocket. Thus the presence of the benzene ring in MCSS phenol eliminates such a misleading result. The ring also adds several kcal/mol to the favorable van der Waals component of the group interaction energy.

There is second, smaller lobe of GRID density at the center of the pocket, also with no overlapping MCSS minima in Figure 7. In this case, however, MCSS does place two slightly higher energy minima (#115, 116) with their hydroxyls at that location. Minima #115 (E = −10.39 kcal/mol) and #116 (−10.15 kcal/mol) were examined further. These two minima are very close in position. The vacuum-minimized MCSS phenol group is entirely planar. Apart from its hydroxyl hydrogen (which is bent slightly out of plane), minimum #116 also is planar, and thus this minimum has almost no strain energy (0.37 kcal/mol). Also, its nonbonded interaction energy with the protein is almost entirely due to van der Waals interactions (external van der Waals energy = −9.76 kcal/mol; vacuum reference energy = −0.39 kcal/mol) . In contrast, the O–H bond axis in minimum #115 is shifted considerably out of the ring plane (its angle with the ring plane is 67.4 deg) to permit donation of a hydrogen bond to the phenolic oxygen of Tyr 1159. Thus this minimum has a significant strain energy (+3.53 kcal/mol), mostly due to this dihedral strain. However, this energy cost is compensated for by improved electrostatic interactions with the protein, which correspond to the hydrogen bond. The GRID density in this region corresponds to minimum #115 in that the GRID probe evaluated at the positions of #115 and #116 indicates a hydrogen bond with Tyr 1159 O. The MCSS results reveal that placing the hydroxyl group in this position, to allow hydrogen bonding, introduces considerable dihedral strain. This may be seen as an example of the specificity that can be gained from hydrogen bonding interactions, and the potential energetic cost of such specificity. In this case, an isoenergetic conformation is available which lacks the hydrogen bond, but has a more ideal geometry. Minimum #116 is an example of the 'affinity' resulting from multiple, less specific van der Waals interactions.

Several MCSS phenol minima located around the exterior (hydrophilic) pocket entrance are approximately isoenergetic with minima found in the pocket interior. However, while the phenol minima on the exterior usually derive most of their interaction energy from hydrogen bonds, those in the interior consistently fail to form hydrogen bonds; rather, their interaction energy derives mostly from van der Waals interactions. It is notable that the GRID functional map for the aromatic hydroxyl probe often identifies sites around the pocket entrance but not in the pocket interior, despite the presence of nearly isoenergetic MCSS phenol minima at both locations. (This effect was not observed for simpler probes, i.e., methane or water.) Since GRID uses single sphere probes, it only can identify specific interactions (for polar probes), and hence it is not surprising that it fails to identify these interior MCSS minima positions as favorable, as their energy is the cumulation of several (small) van der Waals terms. Chemically realistic functional groups that can account for specific polar interactions as well as for multi-atom dispersive types of interactions and internal strain, are a significant strength of the MCSS method.

The effect of including internal strain is not particularly large for this mostly aromatic system. The ten lowest energy MCSS phenol minima were examined and were planar, although the carbon-oxygen and oxygen-hydrogen bond lengths usually were increased slightly and the C–O–H bond angles decreased slightly from ideal values, to optimize hydrogen bonds formed with the protein. For these MCSS phenol minima, the resulting strain energies ranged from 0.82 to 4.44 kcal/mol. These two energies represent 2.6% and 14.1% of the total interaction energy, respectively.

As noted previously, the GRID interaction energy includes only external nonbonded interactions. Thus for the aromatic hydroxyl probe, the closest analogue of the GRID interaction energy is given in MCSS by the sum of external nonbonded interactions of the phenol oxygen and its hydrogen, i.e., the *external energy* of the hydroxyl group. In general, this energy sum dominates the total interaction energy for the entire MCSS phenol group since these two atoms have large partial charges (q = −0.65 and 0.40 for O and H, respectively), while the remaining phenol atoms are neutral apart from the adjacent carbon, CZ (q = 0.25), which completes the charged group. It was noted ear-

lier that considering one or more atoms of a charge group apart from the others can lead to 'unbalanced' results for electrostatic interactions. A few cases are seen in which the external energy of the hydroxyl group is positive, though when the CZ atom also is included, the energy sum always becomes favorable. The correlation of the phenol MCSS energy with the GRID aromatic hydroxyl probe at the same positions is 0.457; when the external energy of the hydroxyl group is used, the correlation is 0.490. Thus, the difference is not important in this case.

The MCSS phenol group and the GRID aromatic hydroxyl probe also were studied using the src SH3 system. The analysis was limited to the surface of the SH3 domain which interacts with other proteins. Over this region, the MCSS minima are distinctly clustered, corresponding to interactions with exposed side chains. The lowest-energy minimum was −29.42 kcal/mol. The GRID map also characteristically clusters around exposed side chains; the lowest-energy GRID point is −12.65 kcal/mol. Figure 8 shows the sixty lowest-energy MCSS phenol minima, with the corresponding GRID map. The results are qualitatively similar to those seen in the poliovirus system; e.g., occasionally the GRID probe penetrates more closely into the protein surface, and in some cases relatively low-energy MCSS minima are not identified by a GRID contour. This similarity is significant given the very different nature of the two binding sites under study, and suggests the generality of the results obtained here.

Cyclohexane

The MCSS cyclohexane group in the hybrid representation consists of six extended-atom carbons and hence it was compared to six GRID methane probes, i.e., at each of the six carbon positions of a given cyclohexane minimum, the GRID methane interaction energy was evaluated. (This is comparable in concept to what GROUP does. GROUP is a part of the GRID program suite which works by fitting GRID maps together to represent larger fragments. However, it currently requires that at least three hydrogen bonding polar atoms are present in the fragment and thus is not applicable to the cases studied here, cyclohexane and phenol.) These six GRID interaction energies were added to give an estimate of the external nonbonded interactions in cyclohexane. However, this sum substantially overestimates the nonbonded interactions of a multi-atom structure, such as cyclohexane, because it implicitly includes additional hydrogens, which contribute appreciably to the total van der Waals energy. This effect poses a limitation on the use of GRID single spheres to model multi-atom systems like cyclohexane or benzene.

As is the case for phenol, the MCSS cyclohexane group accounts for conformational effects that contribute to the interaction energy. The cyclohexane MCSS energy and the cyclohexane external energy (i.e., the sum of all external nonbonded interactions) were very similar for the twenty-two lowest-energy minima. [(Note that the calculated external energy does not include the vacuum reference energy, which for cyclohexane is very small (E = 0.011 kcal/mol).)] For the remaining minima, the external energy often exceeded the interaction energy in magnitude, though always by around 6.0 kcal/mol. These results are consistent with the observed conformations of these cyclohexane minima: the lowest energy minima are in the chair conformation and the higher energy minima often are in the twist-boat conformation, which is approximately 6.0 kcal/mol higher in energy. This result and the previous ones for phenol demonstrate the ability of MCSS to account for changes in the conformation, which are relevant to the study of large, flexible groups.

Ligand-protein interactions

The ability of the MCSS and GRID programs to find the binding site positions of functional groups in a known ligand is one way to test the methods. The X-ray structure of poliovirus complexed with the antiviral drug R78206 [16] was used for this purpose. For a program like GRID, which uses single sphere probes individually to represent functionalities in a ligand, the influence of neighboring functionalities in the ligand cannot be accounted for. In a large, multi-functional ligand like R78206, both internal and external interactions can have significant, and often countervailing, influences on the ligand position and orientation. For this reason, functional group searches involving larger, more chemically realistic groups are preferred. R78206 consists of a methylpyradizinyl-piperidine group connected by a short alkyl chain to an ether-linked benzoate group (Figure 9). Hence MCSS functional group maps for methylpyradizine, methylpyradazinyl-piperidine, and phenol were calculated for the P3/Sabin structure, along with the corresponding GRID probe maps. The GRID probes examined include the aromatic carbon, ether oxygen,

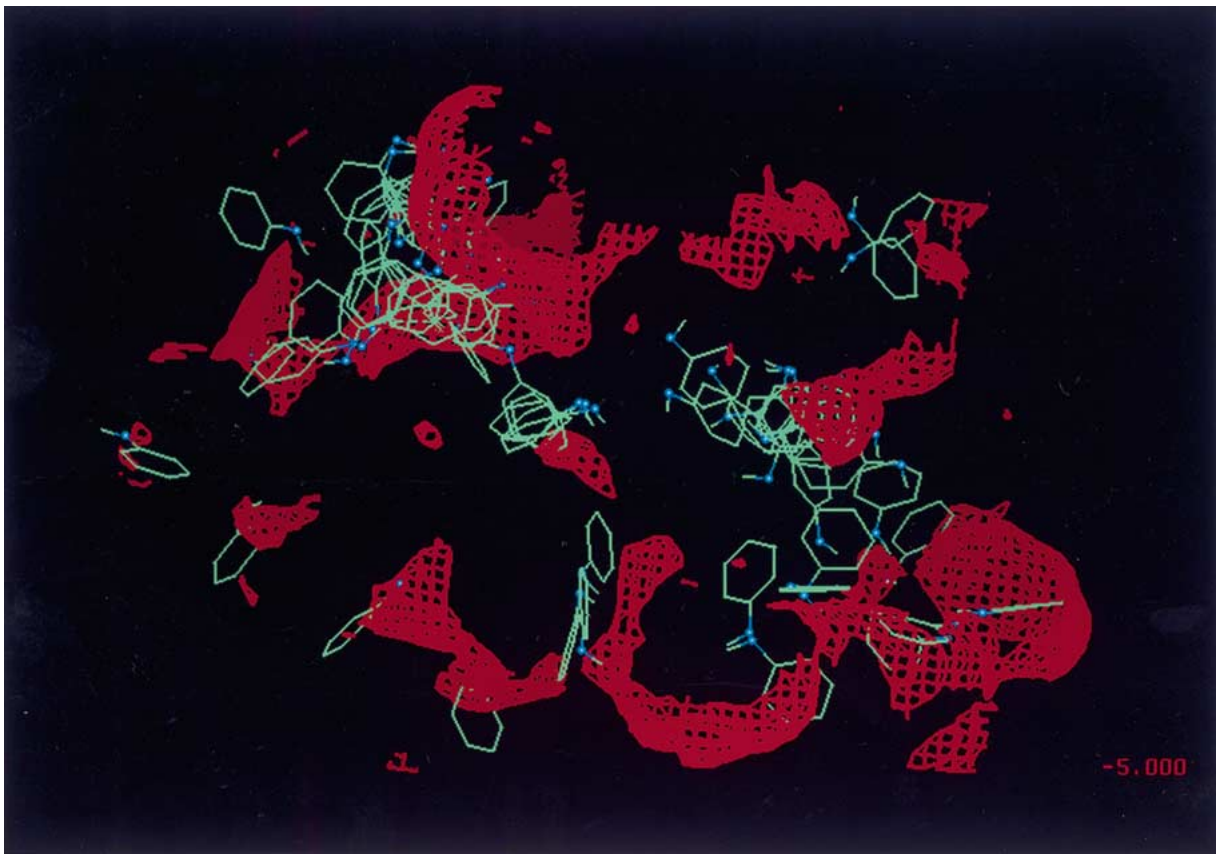

Figure 8. A comparison of the MCSS phenol minima for the binding surface of the src SH3 structure and the corresponding GRID map for an aromatic hydroxyl probe, contoured as indicated. The MCSS minima with an energy less than −13.0 kcal/mol are shown; blue dots indicate the oxygen atoms of these phenol minima.

sp2 carboxy oxygen, methane, and sp2 lone-pair nitrogen probes; these probes correspond to the most important atoms present in the MCSS groups. Since each MCSS group minimum represents a local minimum on the group potential energy surface, it was expected that the resulting MCSS fragment maps would identify positions near, but not necessarily superimposed upon, the experimental structure; the latter has a somewhat different potential surface because the position of each fragment is influenced by the other atoms in the ligand, as well as solvent.

In comparison with the crystal structure, we examine MCSS groups, representing a given fragment, in the neighborhood of that part of the ligand. In addition, there are, of course, other minima for the same MCSS group which are far away because the binding pocket is large; e.g., for methylpyradizine, there are minima found in basically all locations seen for phenol (cf., Figure 7). One low-energy MCSS methylpyradizine minimum deep in the poliovirus capsid pocket (i.e., the region of the uppermost triangle in Figure 7) is #41 (E = -13.42 kcal/mol), which is close to the observed position of this group in R78206, though it is shifted toward the piperidine ring (all-atom rmsd = 1.44 Å). A second, lower-energy minimum (#32, −14.97 kcal/mol) also is nearby (all-atom rmsd = 2.77 Å), though it is shifted deeper into the pocket and has its methyl group pointing in the wrong direction relative to the observed structure. When the MCSS group was extended to included the adjacent piperidine ring, the lowest energy minimum in the deep interior of the pocket (#98, E = −11.71 kcal/mol) overlapped well with the experimentally determined position of the group in R72806 (Figure 10), except that it places the nitrogens of the pyradizine ring on the opposite side of the binding pocket relative to the X-ray structure [16]. The experimental electron density cannot distinguish between the two conformations. The next lowest energy minimum in this region of the pocket (#102, E = −11.33 kcal/mol) has the

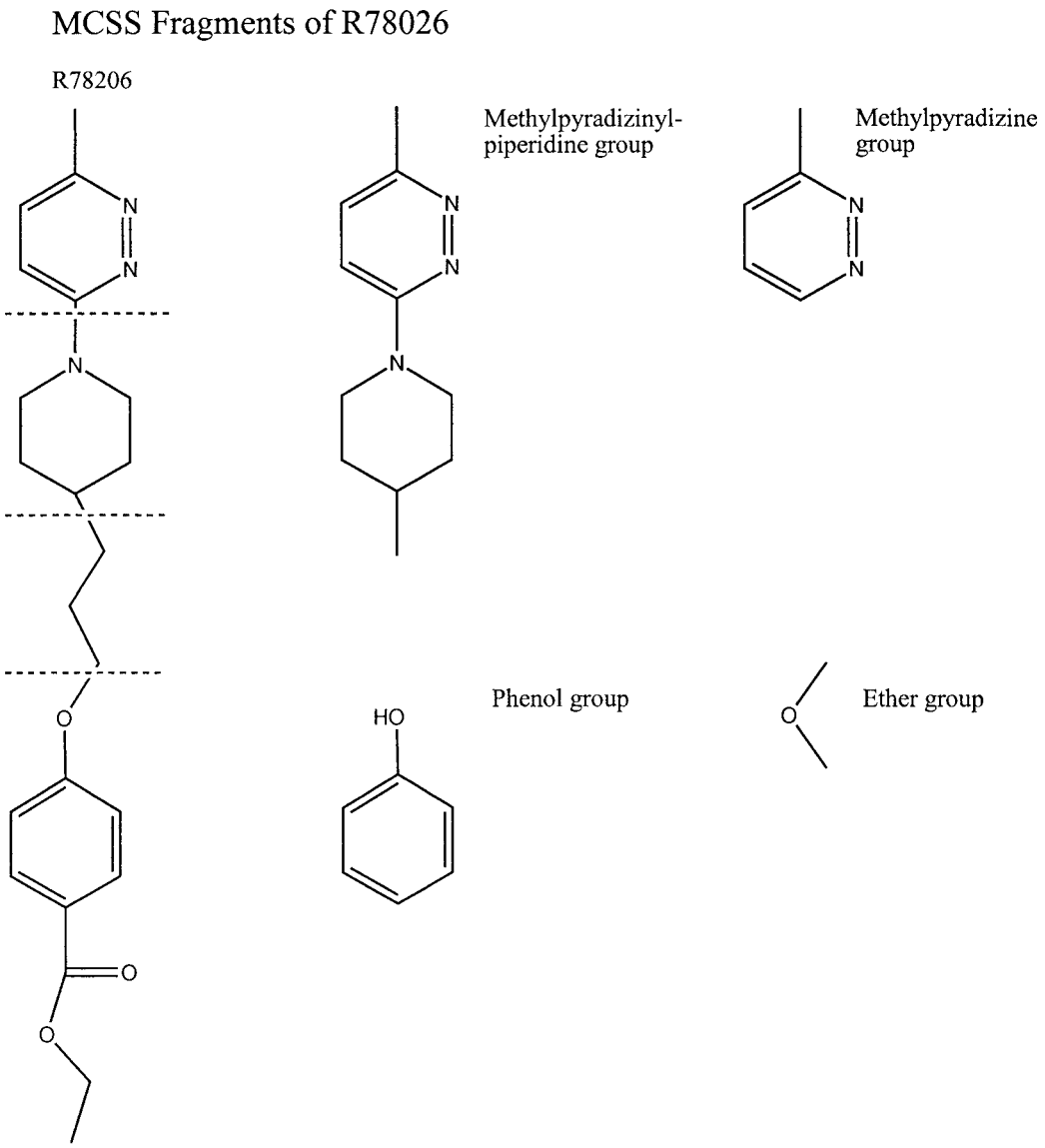

Figure 9. The structure of Janssen compound R78206 and of several fragments used as MCSS groups.

pyradizine ring flipped, indicating that the two alternative conformations are close in energy. The GRID probe N:=, which represents an sp2 nitrogen with one lone pair, also places the nitrogens on the same side of the binding pocket as MCSS minimum #98 (Figure 10). In the case of GRID, however, the other side of the pocket is not identified until the map is contoured at such a high level that it outlines the entire van der Waals surface of the binding pocket (this occurs for all probes at around the −2.0 kcal/mol contour).

This example emphasizes several interesting aspects of ligand binding in this pocket. At the buried apex of the binding pocket (arrow in Figure 10), GRID usually indicates that all probes, both polar and nonpolar, are favorable. MCSS also generally finds minima in this area irrespective of the group examined. This favorable and non-discriminating binding exists in part due to multiple potential hydrogen bonding partners (include backbone atoms as well as side chain atoms). Proceeding toward the pocket entrance, one enters a hydrophobic region bound largely by the aromatic rings of Phe 1134 on one side and Tyr 1159 on the other. These two rings are nearly parallel, and thus constrain the piperidine ring of

R78206 which is stacked between them to be oriented in the same way. In the vacuum-minimized structure of methylpyridazinyl-piperidine, the pyradizine and piperidine rings are almost orthogonal, and the piperidine ring is in the chair conformation. However, this configuration of methylpyridazinyl-piperidine is prohibited by the geometry of the binding pocket. Thus, in the R78206-P3/Sabin structure, the piperidine ring is rotated such that it is nearly coplanar with pyradizine; in addition, the chair conformation is 'flattened' at the end attached to pyradizine. The conformation of minimum #98 is similar, though the direction of the piperidine ring pucker is opposite. A MCSS cyclohexane map does not locate the position of the piperidine ring, but rather places minima (none of which are similarly 'flattened') above and below this site. These considerations make it clear why the extended MCSS group is required to reproduce the observed positions in the drug structure. In contrast to the results obtained for the methylpyradizine and cyclohexane MCSS groups, the methylpyradizinyl-piperidine map indicates no relevant minima deeper than the crystallographically observed position.

There also is an MCSS phenol minimum (#41) that is in agreement with the position of the central ether-linked benzene unit (Figure 10), again the lowest energy phenol minimum in that region. By contrast, the GRID ether oxygen probe failed to highlight the relevant atomic position of oxygen in R78206. However, the GRID aromatic carbon probe was successful in selectively identifying the carbons of the pyradizine group and the central aromatic ring, and the GRID sp2 carboxy oxygen atom probe identified one of the two carboxyl oxygen positions. The success of this last probe is consistent with the earlier observation that GRID is best at identifying polar interactions which, in the simplest approximation, are pair interactions and thus can be discerned via single sphere probes. Similarly, it is not surprising that a highly hydrophobic fragment like the aromatic carbon probe is successful here, while less successful is a probe of intermediate polarity (e.g., ether oxygen), whose electronic properties are more apt to be influenced by its neighbors.

Concluding discussion

A detailed comparison has been made of two methods (GRID and MCSS) which are used in ligand design to find functional group positions in the binding sites of targets with known structure. Functional groups ideally are chemically realistic fragments that can be readily synthesized and connected to other functional groups or lead compounds. Although the overall aims of the two methods are similar, there are significant differences in their execution.

The GRID method [1, 9, 10] finds positions of low energy, mainly for small functional groups which are often represented by single sphere probes. Thus the results are of primary interest for attaching small functional groups to known ligands, when the required orientation of the group is largely predetermined by the structure of the ligand [9, 10]. The low energy positions are found by contouring the probe maps to determine the relative minima, whose positions suggest sites where the lead compound might be modified. Both the location of a relative minimum and its energy relative to other probes are important for this purpose; i.e., the chosen probe must be capable of being connected to the template and it should be lower in energy than other probes at the same location.

The MCSS method determines the optimal binding positions and orientations for both small (e.g., water) and larger (e.g., aromatic) functional groups. The explicit multi-atom structure of MCSS groups (e.g., phenol, cyclohexane, methylpyradizine) results in minima reflecting a balance between highly specific, polar interactions, (e.g., hydrogen bonds), less specific van der Waals (hydrophobic) interactions, and conformational strain. The latter two usually are significant only as multi-atom effects and thus are largely neglected by GRID; e.g., the dispersion interaction involving several atoms can be comparable in energy to a typical hydrogen bond.

Since MCSS can be used for the same purpose as that described for GRID, we have compared the two methods with respect to the results obtained for small molecular probes. The smallest MCSS nonpolar and polar probes (i.e. methane and water) were compared with the corresponding sphere models in GRID. The methane results were very similar both qualitatively and quantitatively, while the water results were similar qualitatively, but less so quantitatively.

In addition, we considered larger MCSS groups (e.g., phenol) in which one or a few heteroatoms were expected to have a decisive influence on the optimum orientation. In general, determining the orientation requires simultaneous optimization of multiple degrees of freedom because the groups are flexible. In the published example where GRID was used for *de novo* design, namely that of a thymidylate synthetase in-

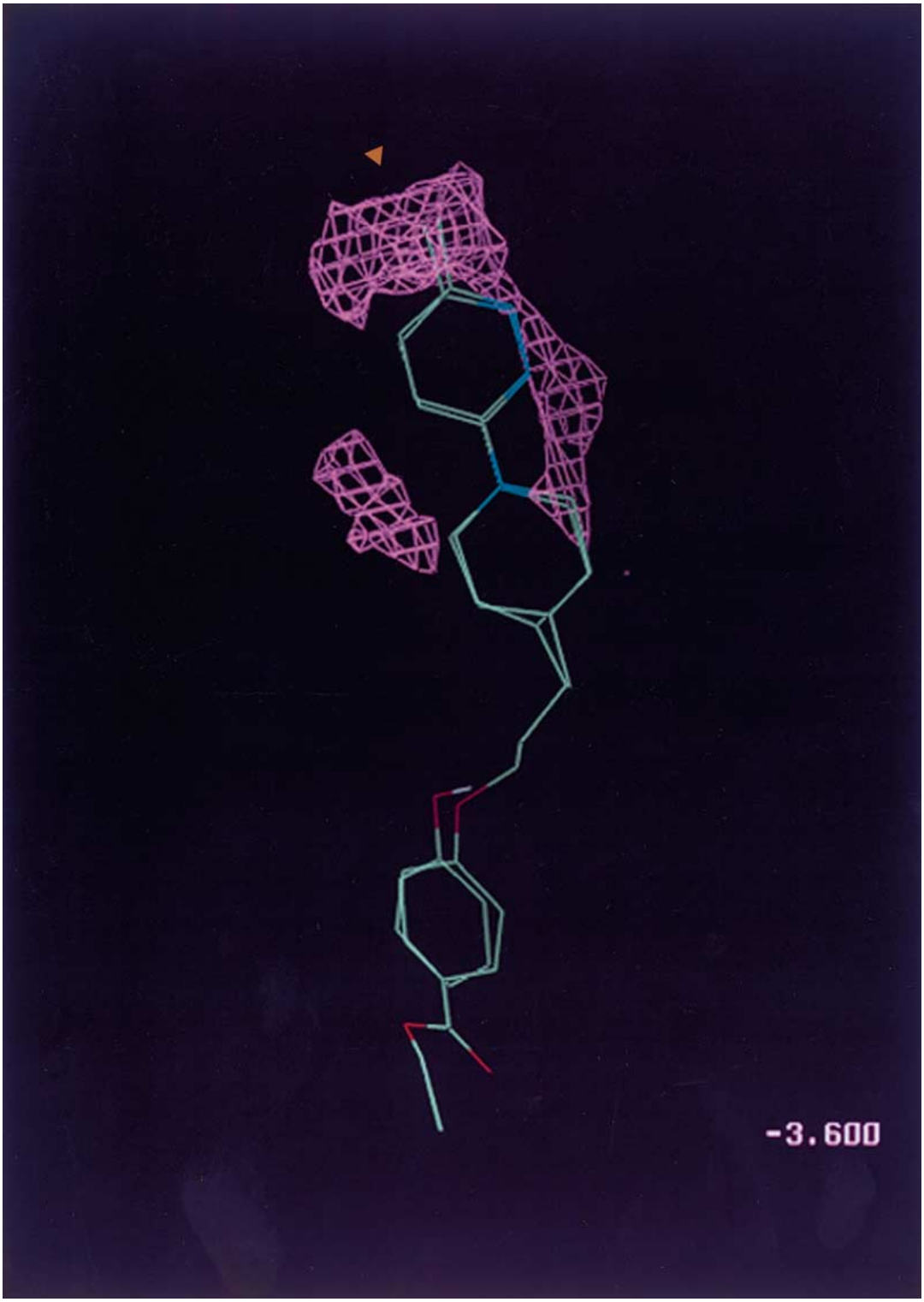

Figure 10. Superposition of the R78206/P3-Sabin poliovirus complex structure (only R78206 is shown) with the lowest energy MCSS methylpyradizinyl-piperidine minimum (#98) at that end of the pocket, and the GRID map for the sp2 lone-pair nitrogen probe in this region; also shown is MCSS phenol minimum #41, which overlaps well with the central ring of R78206. (Note that the R78206 structure has been drawn with the pyradizine nitrogens placed on the opposite side relative to the published x-ray structure; see text for details.)

hibitor [11], the GRID aromatic probe was found to be favored where the pteridine moiety (common to antifolates) binds. This finding motivated the introduction of a naphthalene group to replace pteridine. Due to its aromatic character, naphthalene can be assumed to be planar so optimizing the internal degrees of freedom is not important. In many other examples, however, multi-atom structures are flexible and their conformational energies play a role. MCSS is designed for such situations, while GRID is not. The GROUP module of GRID allows for representation of multi-atom probes, by combining the results for single-sphere probes, but it does not explicitly consider ligand strain effects, and thus is expected in general to overestimate the binding affinity (cf. cyclohexane results).

The results obtained in this report indicate that there is qualitative agreement between the MCSS and GRID results. All MCSS and GRID functional group maps examined were similar, in the sense that most MCSS minima are found within or near the density peaks observed in a multi-contoured display of the GRID results. Despite this general agreement, differences emerge when the GRID probes are evaluated at the exact locations of the MCSS minima. For methane, the two methods compare very well, as they should because methane is represented as a sphere with a very similar Lennard–Jones potential in both methods. Methane is the only MCSS group represented as a single sphere probe. The methane results are representative of how van der Waals interactions in general compare in the two methods.

For the polar probes (e.g., water, methanol) the form of the empirical energy function used in the two methods is quite different; it is this factor which contributes most to the observed differences in the energy values. In MCSS, the electrostatic term accounts for nonbonded interactions other than van der Waals, while GRID also includes an explicit hydrogen bonding term. Since the GRID atomic partial charges are small relative to those used in MCSS, the GRID hydrogen bonding term generally dominates the interaction energy if a hydrogen bond exists between the probe and protein. The GRID polar energy thus is based on the hydrogen bond contribution. However, because these bonds are formed according to certain criteria, a slight change in position can significantly alter the GRID hydrogen bonding energy, as a possible protein acceptor moves into or out of the allowed geometric range. No such behavior was found in the MCSS energies. This underscores the need to account for electrostatic interactions that do not qualify as hydrogen bonds in GRID. The GRID electrostatic term is usually very small; in the case of neutral probes (such as water), it is identically zero. MCSS circumvents this difficulty by not using directional interactions and summing over all terms that arise from atomic partial charges. Hydrogen bonding interactions are accounted for in the self-consistent parametrization of the potential function [28]. As a result of such differences in the respective potential functions, the MCSS and GRID interaction energies for the water probe differed considerably, and often irregularly. Nonetheless, the resulting MCSS and GRID water maps were qualitatively similar. Considering the types of applications of the two approaches in drug design, this is perhaps more important than their quantitative differences. The results obtained with the water probe show how the treatment of polar interactions differs in the two methods.

In contrast to methane and water, most functional groups in the MCSS library correspond to larger systems. For these systems, the MCSS results differ qualitatively from those of the GRID single sphere probes; e.g. MCSS identifies additional binding sites and excludes restricted sites. The poliovirus binding pocket, which is used as a model system in the present study, is commonly described as hydrophobic. However, it contains both hydrophobic and hydrophilic residues, and a diverse set of side chain and main chain atoms line its surface. Comparing MCSS groups (such as phenol and methylpyradizine) with the corresponding GRID polar probes, the GRID functional group map characteristically identifies sites at the hydrophilic entrance to the pocket but not in the pocket interior; isoenergetic MCSS minima are present in both regions. The multi-atom structure of MCSS groups results in minima reflecting a balance between several types of interactions. The relevance of these effects is evident in the earlier finding [13] that complex MCSS groups such as phenol, indole, and imidazole are more favored within the poliovirus binding pocket than groups such as benzene, toluene and propane, or water and methanol, that only have one type of interaction with the protein. MCSS also allows the binding of several groups in noncovalent association to be examined. For example, a water molecule associated with another group has been treated together as a single functional group [13]; if the combination is energetically favorable (e.g., Mg^{+2}–H_2O), the two groups remain together during minimization.

The speed of GRID offers an advantage if the binding site is unknown and the entire macromolecule must be searched. In such cases, random placement and minimization of MCSS groups over the required region can be quite expensive computationally. One possibility would be to use GRID to identify the relevant binding regions and perhaps to suggest the types of functional groups which are likely to be important. Particularly for smaller probes, this could be very useful; e.g., hydrophobic regions are readily identified in a GRID contour map, which connects broad regions stretching across the protein surface. MCSS could be applied subsequently to give more detailed results concerning the best positions and orientations for multi-atom groups in the region suggested by a GRID search. If a drug discovery effort aims primarily to optimize an existing lead molecule, both GRID and MCSS appear to be suitable methods. However, for the *de novo* design of larger ligands with several functional groups, the MCSS method is the better approach. It determines the positions and orientation required for efficient construction of ligands with approaches like HOOK [30] and DLD [31]. MCSS is of interest also because of its generality; e.g., the method can be used for composite functional groups, such as Mg^{+2}–H_20, and can be employed to study flexible binding sites, as well as flexible ligands.

Acknowledgements

Supported in part by NIH grant AI32480 to J.M.H., a grant from the National Science Foundation to M.K., and a Harvard-Armenise Foundation Fellowship to D.J-M. The authors thank Erik Evensen for many stimulating discussions. All computations were done on Silicon Graphics O2 workstations.

References

1. Goodford, P.J., J. Med. Chem., 28 (1985) 849.
2. Boobbyer, D.N.A., Goodford, P.J., McWhinnie, P.M. and Wade, R.C., J. Med. Chem., 32 (1989) 1083.
3. Wade, R.C., Clark, K.J. and Goodford, P.J., J. Med. Chem., 36 (1993) 140.
4. Wade, R.C. and Goodford, P.J., J. Med. Chem., 36 (1993) 148.
5. Evensen, E., Joseph-McCarthy, D. and Karplus, M., *MCSSv2*, Harvard University, 1997.
6. Miranker, A. and Karplus, M., Proteins, 11 (1991) 29.
7. Caflisch, A., Miranker, A. and Karplus, M., J. Med. Chem., 36 (1993) 2142.
8. Caflisch, A. and Karplus, M., Perspectives in Drug Discovery and Design, 3 (1995) 51.
9. Jedrzejas, M.J., Singh, S., Brouillette, W.J., Air, G.M. and Luo, M., Proteins, 23 (1995) 264.
10. vonItzstein, M., Dyason, J., Oliver, S., White, H., Wu, W., Kok, G. and Pegg, M., J. Med. Chem., 39 (1996) 388.
11. Appelt, K., Bacquet, R.J., Bartlett, C.A., Booth, C.L.J., Freer, S.T., Fuhry, M.A.M., Gehring, M.R., Herrmann, S.M., Howland, E.F., Jansen, C.A., Reddy, M.R., Reich, S.H., Schoettlin, W.S., Smith, W.W., Varney, M.D., Villafranca, J.E., Ward, R.W., Webber, S., Webber, S.E., Welsh, K.M. and White, J., J. Med. Chem., 34 (1991) 1925.
12. Goodford, P.J., GRID User Manual, Edition 16.
13. Joseph-McCarthy, D., Hogle, J.M. and Karplus, M., Proteins, 29 (1997) 32.
14. Hogle, J.M., Chow, M. and Filman, D.J., Science, 229 (1985) 1358.
15. Filman, D.J., Syed, R., Chow, M., Macadam, A.J., Minor, P.D. and Hogle, J.M., EMBO J., 8 (1989) 1567.
16. Grant, R.A., Hiremath, C.N., Filman, D.J., Syed, R., Andries, K. and Hogle, J.M., Curr. Biol., 4 (1994) 784.
17. Hiremath, C., Grant, R.A., Filman, D.J. and Hogle, J.M., Acta Cryst., D51 (1995) 473.
18. Hiremath, C.N., Filman, D.J., Grant, R.A. and Hogle, J.M., Acta Cryst., D53 (1997) 558.
19. Rossmann, M.G., Arnold, E., Erickson, J.W., Frankenberger, E.A., Griffith, J.P., Hecht, H.-J., Johnson, Kamer, G., Luo, M., Mosser, A.G., Rueckert, R.R., Sherry, B. and Vriend, G., Nature, 317 (1985) 145.
20. Kim, K.H., Willingmann, P., Gong, Z.X., Kremer, M.J., Chapman, M.S., Minor, I., Oliveira, M.A., Rossmann, M.G., Andries, K., Diana, G.D., Dutko, F.J., McKinlay, M.A. and Pevear, D.C., J. Mol. Biol., 230 (1993) 206.
21. Badger, J.; Minor, I., Kremer, M.J., Oliveira, M.A., Smith, T.J., Griffith, J.P., Guerin, D.M.A., Krishnaswamy, S., Luo, M., Rossmann, M.G., McKinlay, M.A., Diana, G.D., Dutko, F.J., Fancher, M., Rueckert, R.R. and Heinz, B.A., Proc. Natl. Acad. Sci. USA, 85 (1988) 3304.
22. Badger, J., Minor, I., Oliveira, M.A., Smith, T.J. and Rossmann, M.G., Proteins, 6 (1989) 1.
23. Feng, S., Kapoor, T.M., Shirai, F., Combs, A.P. and Schreiber, S.L., Chem. Biol., 3 (1996) 661.
24. MacKerell, A.D., Bashford, D., Bellot, M., Dunbrack, R.L., Evanseck, J.D., Field, M.J., Fischer, S., Gao, J., Guo, H., Ha, S., Joseph-McCarthy, D., Kuchnir, L., Kuczera, K., Lau, F.T.K., Mattos, C., Michnick, S., Ngo, T., Nguyen, D.T., Prodhom, B., Reiher, W.E., Roux, B., Schlenkrich, M., Smith, J.C., Stote, R., Straub, J., Watanabe, M., Wiorkiewicz-Kuczera, J., Yin, D. and Karplus, M., J. Phys. Chem. B, 102 (1998) 3586.
25. Brünger, A.T., Kuriyan, J. and Karplus, M., Science, 235 (1987) 458.
26. Brooks, B.R., Bruccoleri, R.E., Olafson, B.D., States, D.J., Swaminathan, S. and Karplus, M., J. Comp. Chem., 4 (1983) 187.
27. Elber, R. and Karplus, M., J. Am. Chem. Soc., 112 (1990) 9161.
28. Neria, E., Fischer, S. and Karplus, M., J. Chem. Phys., 105 (1996) 1902.
29. Halgren, T.A., J. Comput. Chem., 17 (1996) 490.
30. Eisen, M.B., Wiley, D.C., Karplus, M. and Hubbard, R.E., Proteins, 19 (1994) 199.
31. Miranker, A. and Karplus, M., Proteins, 23 (1995) 472.
32. Tsang, S.K., Cheh, J., Isaacs, L., Joseph-McCarthy, D., Choi, S.K., Pevear, D.C., Whitesides, G.M. and Hogle, J.M., Chem. Biol., 8 (2001) 33.